Laboratory of Bio-Functional Molecular Chemistry[1], Graduate School of Pharmaceutical Sciences, Osaka University, Osaka; School of Pharmaceutical Sciences[2], Teikyo Heisei University, Chiba, Japan

A toxicological evaluation of a claudin modulator, the C-terminal fragment of *Clostridium perfringens* enterotoxin, in mice

H. Suzuki[1], M. Kondoh[1], X. Li[1], A. Takahashi[1], K. Matsuhisa[1], K. Matsushita[1], Y. Kakamu[1], S. Yamane[1], M. Kodaka[1], K. Isoda[2], K. Yagi[1]

Received December 2, 2010, accepted December 29, 2010

Masuo Kondoh, Ph.D., Kiyohito Yagi, Ph.D., Laboratory of Bio-Functional Molecular Chemistry, Graduate School of Pharmaceutical Sciences, Osaka University, Suita, Osaka 565-0871, Japan
masuo@phs.osaka-u.ac.jp; yagi@phs.osaka-u.ac.jp

Pharmazie 66: 543–546 (2011) *doi: 10.1691/ph.2011.0365*

Tight junctions (TJs) maintain cellular polarity between the apical and basolateral region of epithelial cells. Claudin, a tetra-transmembrane protein, plays a pivotal role in the barrier function of TJs. We previously found that a claudin modulator, the C-terminal fragment of *Clostridium perfringens* enterotoxin (C-CPE), may be a promising candidate for improving the mucosal absorption of drugs. C-CPE is a fragment of enterotoxin, and putative CPE claudin receptors are highly expressed in liver and kidney. The safety and antigenicity of C-CPE must be evaluated for future clinical application. Therefore, we evaluated whether C-CPE administration in mice leads to tissue injury or production of antibodies. Intravenous administration of C-CPE at 5 mg/kg, which is a more than 25-fold higher dose than that used in a murine mucosal absorption model, did not increase biochemical markers of liver and kidney injury even after 11 injections once a week. Nasal C-CPE administration (2 mg/kg) once a week for 11 administrations also did not increase these biochemical markers, but 6 administrations of C-CPE resulted in elevation of C-CPE-specific serum IgG. These results indicate that development of a less antigenic claudin modulator will be essential for future clinical application of a C-CPE-based mucosal absorption enhancer.

1. Introduction

The use of biologics, such as antibodies, peptides, and nucleic acids, in new drugs is becoming increasingly prominent. Biologics are biodegradable and poorly absorbed in the mucosa, and therefore they are often employed as injectable drugs. The development of a non-invasive system for delivery of drugs across the mucosal epithelium would improve quality of life and patient compliance. Since orally administered drugs can be degraded by digestive enzymes and first pass effects in the liver, developing ways to administer drugs through nasal and pulmonary transmucosal absorption has a high priority. However, passing biologics across the mucosal epithelium is extremely difficult because the mucosa's primary function is as a physical and biological barrier preventing the entry of pathogens and toxic substances into the body.

Epithelial cell sheets develop intercellular junctions to prevent the free movement of solutes between sheets. Adjacent epithelial cells adhere to one another via tight junctions (TJ), adherent junctions, and gap junctions. Among these, the TJ plays a key role in sealing the intercellular space and preventing leakage of solutes. Modulation of the TJ barrier has proven to be a promising strategy for enhancement of mucosal drug absorption. Tight junction modulators, such as surfactants, chelators, and nitric oxide donors, have been investigated as potential absorption enhancers since the 1960 s (Aungst 2000; Citi 1992; Engel and Riggi 1969; Tomita et al. 1996).

The detection and development of absorption-enhancers focuses on modulating activity of the TJ barrier. Such enhancers are called "the first generation TJ modulators" (Kondoh et al. 2008). The identification of claudin, a structural and functional TJ component, provided new insight into absorption-enhancers, and led to a TJ-components-based strategy for enhancer development, the second generation TJ modulators. Claudins are ~23 kDa proteins bearing tetra-transmembrane domains and comprise a family of more than 20 members (Furuse and Tsukita 2006). The expression profiles and barrier function of the various claudin family members differ among tissues. For instance, claudins-1 and -5 are critical for epidermal barrier and blood-brain-barrier functions, respectively (Furuse et al. 2002; Nitta et al. 2003). Modulation of the claudin barrier has been proposed as a novel strategy for absorption enhancement (Furuse et al. 1998; Tsukita and Furuse 1998).

Clostridium perfringens enterotoxin (CPE) is a cause of food poisoning in humans (McClane and Chakrabarti 2004). A receptor of CPE is identical to claudin-3/4, and the C-terminal fragment of CPE (corresponding to amino acids 184–319) modulates the TJ barrier by its interaction with claudin-3/4 (Sonoda et al. 1999). We found that the claudin modulator the C-terminal fragment of CPE was 400-fold more potent at enhancing intestinal absorption than a clinically used absorption-enhancer, sodium caprate (Kondoh et al. 2005). However, the C-terminal fragment of CPE did not enhance intestinal absorption of a peptide drug when co-administered (Uchida et al. 2010). The N-terminal truncated fragment (C-CPE), comprising amino acids 194–319, did enhance intestinal, nasal, and pulmonary absorption of a biologically active peptide (Uchida et al. 2010). Thus, C-CPE may be a promising enhancer of mucosal drug absorp-

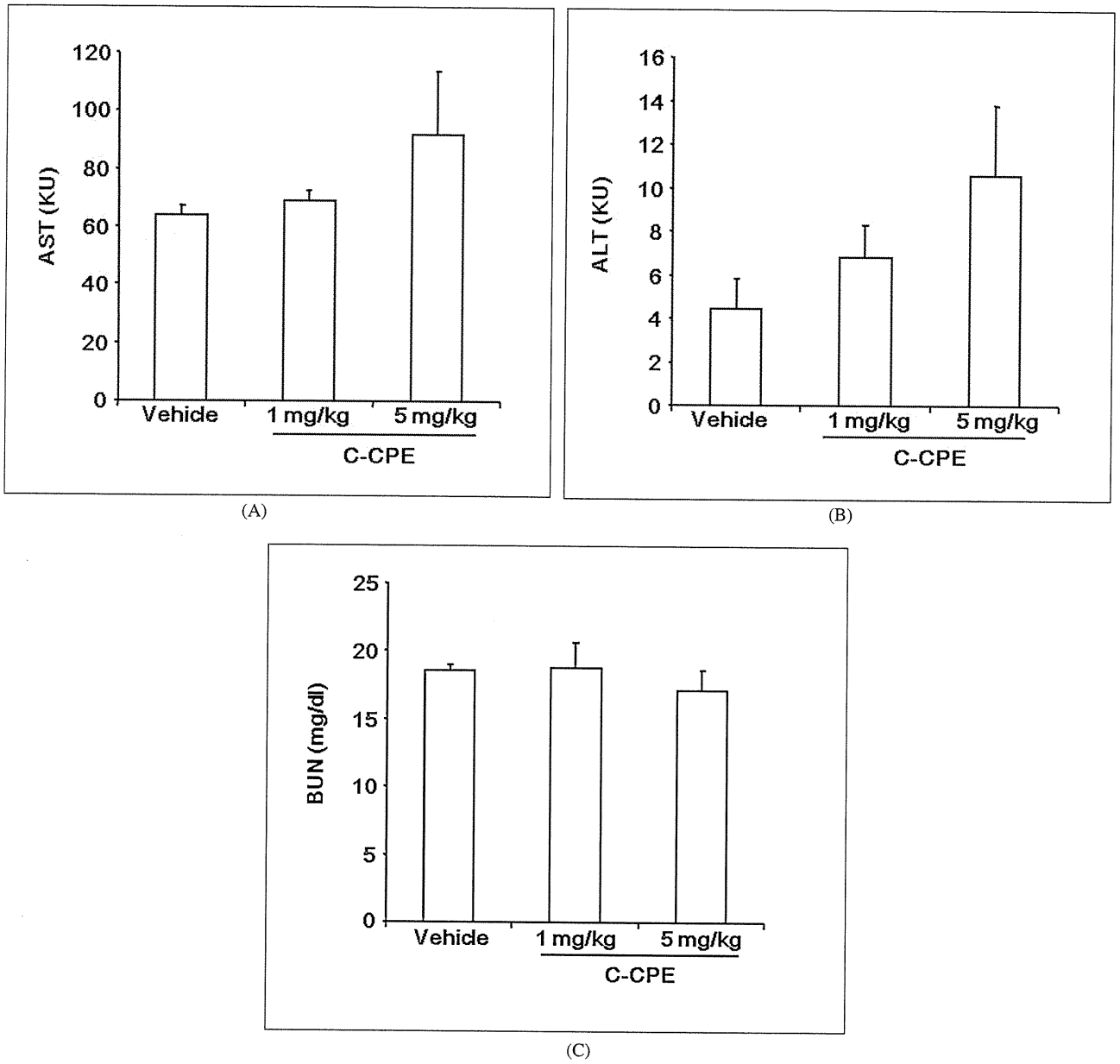

Fig. 1: Effect of systemic injection of C-CPE on biochemical markers for liver and kidney injury. Mice received intravenous injections of C-CPE at 0, 1, or 5 mg/kg once a week for 11 weeks. Blood was recovered 24 h after the last administration of C-CPE. Serum AST (A), ALT (B) and BUN (C) were measured using a commercially available kit as described in the Expreimental section. Data are presented as mean ± SEM (n = 3 or 5)

tion. Although data on safety and antigenicity is critical for any future clinical application of C-CPE, its potential side effects have not been investigated.

In the present study, we investigated the effect of C-CPE administration on liver and kidney tissues in which claudin-3/4 is expressed, as well as studied induction of anti-C-CPE antibodies.

2. Investigations, results and discussion

Administration of C-CPE enhanced the mucosal absorption of dextran with a molecular weight of 20 kDa, indicating that C-CPE (13 kDa) might enter into the systemic flow from the mucosal membrane with drugs (Kondoh et al. 2005). C-CPE constitutes the receptor-binding domain of CPE, and binds to claudin-3 and claudin-4 (Fujita et al. 2000; Katahira et al. 1997). Since claudins-3 and -4 are highly expressed in the liver and kidney (Morita et al. 1999), we evaluated the effect of C-CPE on these tissues. To investigate the potential effects of C-CPE on liver and kidney, we systemically injected C-CPE into mice once a week for 11 weeks and measured biochemical markers of liver (AST and ALT) and kidney (BUN) injury 24 h after the last injection. As shown in Figs. 1A, 1B and 1C, intravenous administration of C-CPE did not affect serum AST, ALT and BUN levels, even at a dose as high as 5 mg/kg. C-CPE was mucosally administered at 0.02–0.4 mg/kg (Uchida et al. 2010). Therefore, even if all C-CPE was absorbed, no side effects in liver or kidney are likely to occur.

Since C-CPE is a polypeptide, its antigenicity could interfere with its clinical use. We therefore investigated whether repeated mucosal administration of C-CPE activates serum C-CPE-specific IgG responses. Mice were surgically operated upon in jejunal and pulmonary absorption studies, and consequently could not be repeatedly treated with C-CPE. Therefore, to investigate the antigenicity of C-CPE following mucosal administration, C-CPE was intranasally administered to mice once a week for 10 weeks. Serum IgG production was monitored every week. C-CPE treatment did not increase C-CPE-specific serum IgG after 4 administrations of C-CPE at 2 mg/kg. However, 6 administrations of C-CPE did cause production of C-CPE-

specific serum IgG (Fig. 2). A dose of 1 mg/kg is equal to that used in a previously published study on mucosal absorption (Uchida et al. 2010). Repeated mucosal administration of C-CPE in our study at twice this dose (2.0 mg/kg) did not increase serum AST, ALT and BUN levels (Figs. 3A 3B and 3C). These findings indicate that while C-CPE does not cause tissue damage at clinically relevant doses, it may be limited in its clinical applications as a mucosal absorption enhancer only by its antigenicity.

There are two potential directions for clinical applications of claudin modulators. The first is preparation of a claudin modulator based on C-CPE. An antigenic determinant assay of CPE revealed that the C-terminal fragment corresponding to amino acids 286–305 was immunogenic (Sugii 1994). Mutating the antigenic domain while maintaining its claudin-binding activity would contribute to development of a low antigenic claudin modulator. In general, smaller peptides are less antigenic. The C-terminal fragment corresponding to amino acids 290–319 constituted the receptor-binding domain of CPE (Hanna et al. 1991). Preparation of a claudin-modulating peptide with low antigenicity and high claudin-modulating activity using this 30 amino acid fragment may lead to a claudin modulator useful as an enhancer of drug absorption.

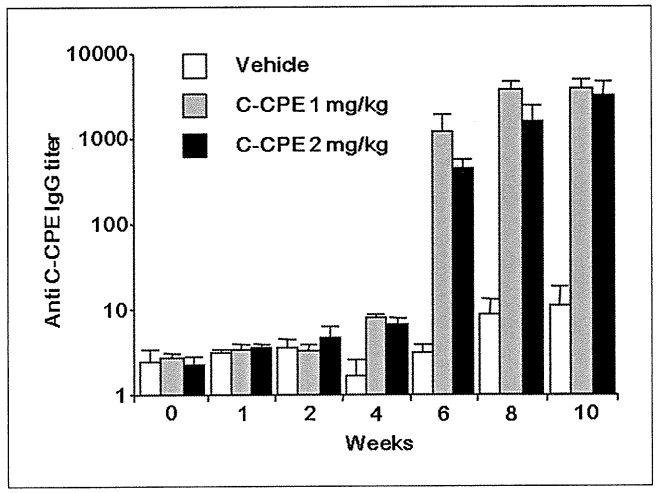

Fig. 2: Effect of mucosal administration of C-CPE on production of anti-C-CPE IgG. Mice received nasal injections of C-CPE at 0, 1, or 2 mg/kg once a week for 10 weeks. Blood was collected each week and serum C-CPE specific IgG levels were measured as described in Materials and methods. Data are presented as means ± SEM (n = 4 or 5)

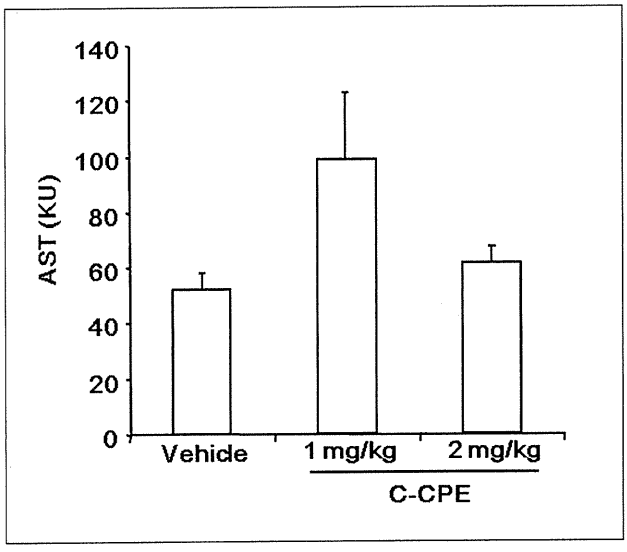

(A)

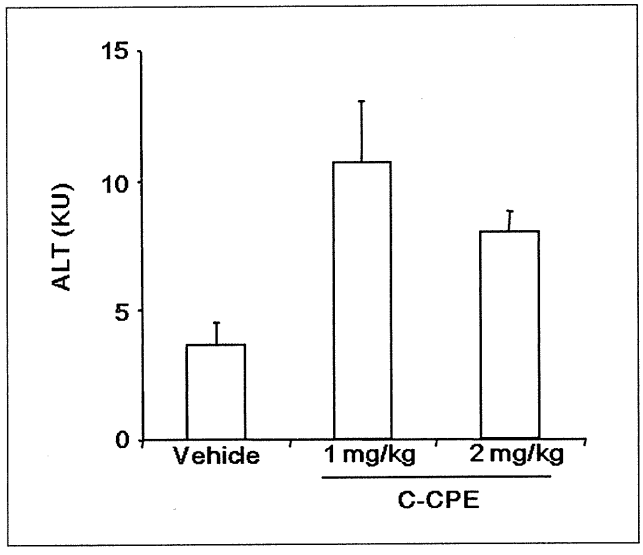

(B)

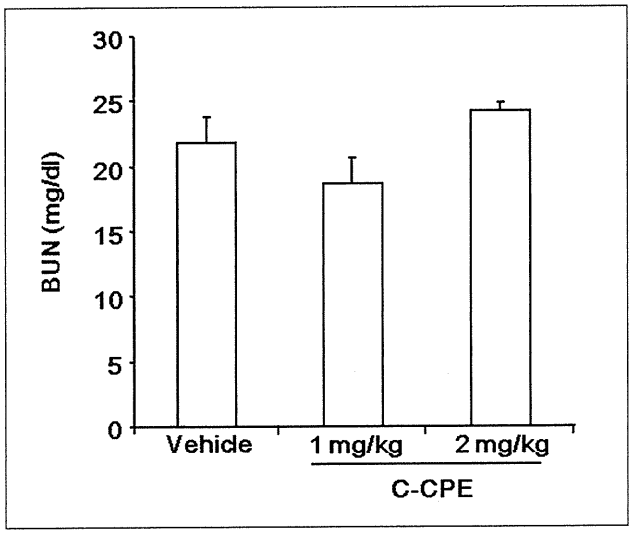

(C)

Fig. 3: Effect of repeated mucosal administration of C-CPE on biochemical markers of liver and kidney injury. Mice were nasally administered with C-CPE at 0, 1, or 2 mg/kg once a week for 11 weeks. Seven days after the last administration, blood was recovered, and serum AST (A), ALT (B) and BUN (C) were measured using a commercially available kit. Data are presented as mean ± SEM (n = 4 or 5)

The second potential direction for clinical applications of claudin modulators lies in the preparation of a human antibody to modulate the claudin-barrier. Claudin is characterized by low antigenicity, and it is therefore difficult to prepare an antibody to bind its extracellular domain (Evans et al. 2007). Recently, Romani et al. successfully prepared a human single-chain antibody to claudin-3, and Suzuki et al. also prepared a monoclonal antibody against claudin-4 (Romani et al. 2009; Suzuki et al. 2009). Development of a humanized antibody against claudin will contribute greatly to the clinical applications of claudin modulators.

In summary, we found that C-CPE administration does not result in significant tissue injury in mice. However, our findings also suggest that discovering a means of reducing C-CPE's antigenicity is critical for continued development of a C-CPE-based claudin modulator useful as an enhancer of drug absorption.

3. Experimentals

3.1. *Animals*

BALB/c female mice (6 wk) were obtained from Shimizu Laboratory Supplies Co., Ltd. (Kyoto, Japan), and were housed in an environmentally controlled room at 23 ± 1.5 °C with a 12-h light/12-h dark cycle. The mice had free access to water and commercial chow (Type MF, Oriental Yeast, Tokyo, Japan). Experimental protocols involving mice were performed according to the ethics guidelines of the Graduate School of Pharmaceutical Sciences, Osaka University.

3.2. *Preparation of C-CPE*

C-CPE was prepared as described previously (Uchida et al. 2010). Briefly, pET16b vector plasmids coding the C-terminal fragment of CPE (amino acids 194–319) were transduced into *E. coli* BL21 (DE3), and protein expression was stimulated by addition of isopropyl-1-thio-β-D-galactoside. Cell lysates were applied to HisTrap™ Chelating HP columns (GE Healthcare, Buckinghamshire, UK), and C-CPE was eluted with imidazole. The solvent was exchanged with phosphate-buffered saline by gel-filtration, and the purified proteins were stored at −80 °C until use. Purification of the proteins was confirmed by sodium dodecyl sulfate-polyacrylamide gel electrophoresis followed by staining with Coomassie Brilliant Blue. C-CPE was quantified by using a BCA protein assay kit (Thermo Fisher Scientific Inc., Rockford, IL) using bovine serum albumin as a standard.

3.3. *Biochemical assay*

C-CPE was administered to mice intravenously or nasally once a week for 11 weeks, and blood was collected from the mice by cardiac puncture one day after the last administration. Serum aspartate aminotransferase (AST), alanin aminotransferase (ALT) levels and blood urea nitrogen (BUN) were measured using commercially available Transaminase-CII and Blood Urea Nitrogen-B Test (WAKO Pure Chemical, Osaka, Japan) kits, respectively.

3.4. *C-CPE-specific antibody production*

C-CPE was administered to mice intravenously or nasally once a week. Serum was collected 7 days after each administration of C-CPE. The titers of C-CPE-specific antibody in serum were determined using an enzyme-linked immunosorbent assay. Briefly, an immunoplate was coated with C-CPE (1 μg/well in a 96-well plate). Ten-fold serial dilutions of samples were added to the wells, followed by reaction with horseradish peroxidase-conjugated anti-mouse IgG. The presence of C-CPE-specific antibodies was determined using TMB peroxide substrate. End point titers were expressed as the dilution ratio, which gave 0.1 above control values obtained for serum of naïve mice at an absorbance of 450 nm.

Acknowledgements: We thank the members of our laboratory for their useful comments and discussion. We would like to thank Dr. Y. Horiguchi (Osaka University, Osaka, Japan) for providing us C-CPE cDNA. This work was supported by a Grant-in-Aid for Scientific Research from the Ministry of Education, Culture, Sports, Science and Technology, Japan (21689006), by a Health and Labor Sciences Research Grants from the Ministry of Health, Labor and Welfare of Japan, by Takeda Science Foundation, by a grant from Kansai Biomedical Cluster project in Saito, which is promoted by the Knowledge Cluster Initiative of the Ministry of Education, Culture, Sports, Science and Technology, Japan. A.T. is supported by Research Fellowships of the Japan Society for the Promotion of Science for Young Scientists.

References

Aungst BJ (2000) Intestinal permeation enhancers. J Pharm Sci 89: 429–442.

Citi S (1992) Protein kinase inhibitors prevent junction dissociation induced by low extracellular calcium in MDCK epithelial cells. J Cell Biol 117: 169–178.

Engel RH, Riggi SJ (1969) Effect of sulfated and sulfonated surfactants on the intestinal absorption of heparin. Proc Soc Exp Biol Med 130: 879–884.

Evans MJ, von Hahn T, Tscherne DM, Syder AJ, Panis M, Wolk B, Hatzioannou T, McKeating JA, Bieniasz PD, Rice CM (2007) Claudin-1 is a hepatitis C virus co-receptor required for a late step in entry. Nature 446: 801–805.

Fujita K, Katahira J, Horiguchi Y, Sonoda N, Furuse M, Tsukita S (2000) *Clostridium perfringens* enterotoxin binds to the second extracellular loop of claudin-3, a tight junction integral membrane protein. FEBS Lett 476: 258–261.

Furuse M, Fujita K, Hiiragi T, Fujimoto K, Tsukita S (1998) Claudin-1 and -2: novel integral membrane proteins localizing at tight junctions with no sequence similarity to occludin. J Cell Biol 141: 1539–1550.

Furuse M, Hata M, Furuse K, Yoshida Y, Haratake A, Sugitani Y, Noda T, Kubo A, Tsukita S (2002) Claudin-based tight junctions are crucial for the mammalian epidermal barrier: a lesson from claudin-1-deficient mice. J Cell Biol 156: 1099–1111.

Furuse M, Tsukita S (2006) Claudins in occluding junctions of humans and flies. Trends Cell Biol 16: 181–188.

Hanna PC, Mietzner TA, Schoolnik GK, McClane BA (1991) Localization of the receptor-binding region of *Clostridium perfringens* enterotoxin utilizing cloned toxin fragments and synthetic peptides. The 30 C-terminal amino acids define a functional binding region. J Biol Chem 266: 11037–11043.

Katahira J, Inoue N, Horiguchi Y, Matsuda M, Sugimoto N (1997) Molecular cloning and functional characterization of the receptor for *Clostridium perfringens* enterotoxin. J Cell Biol 136: 1239–1247.

Kondoh M, Masuyama A, Takahashi A, Asano N, Mizuguchi H, Koizumi N, Fujii M, Hayakawa T, Horiguchi Y, Watanbe Y (2005) A novel strategy for the enhancement of drug absorption using a claudin modulator. Mol Pharmacol 67: 749–756.

Kondoh M, Yoshida T, Kakutani H, Yagi K (2008) Targeting tight junction proteins-significance for drug development. Drug Discov Today 13: 180–186.

McClane BA, Chakrabarti G (2004) New insights into the cytotoxic mechanisms of *Clostridium perfringens* enterotoxin. Anaerobe 10: 107–114.

Morita K, Furuse M, Fujimoto K, Tsukita S (1999) Claudin multigene family encoding four-transmembrane domain protein components of tight junction strands. Proc Natl Acad Sci U S A 96: 511–516.

Nitta T, Hata M, Gotoh S, Seo Y, Sasaki H, Hashimoto N, Furuse M, Tsukita S (2003) Size-selective loosening of the blood-brain barrier in claudin-5-deficient mice. J Cell Biol 161: 653–660.

Romani C, Comper F, Bandiera E, Ravaggi A, Bignotti E, Tassi RA, Pecorelli S, Santin AD (2009) Development and characterization of a human single-chain antibody fragment against claudin-3: a novel therapeutic target in ovarian and uterine carcinomas. Am J Obstet Gynecol 201: 70.e1–70.e9.

Sonoda N, Furuse M, Sasaki H, Yonemura S, Katahira J, Horiguchi Y, Tsukita S (1999) *Clostridium perfringens* enterotoxin fragment removes specific claudins from tight junction strands: Evidence for direct involvement of claudins in tight junction barrier. J Cell Biol 147: 195–204.

Sugii S (1994) Analysis of multiple antigenic determinants of *Clostridium perfringens* enterotoxin as revealed by use of different synthetic peptides. J Vet Med Sci 56: 1047–1050.

Suzuki M, Kato-Nakano M, Kawamoto S, Furuya A, Abe Y, Misaka H, Kimoto N, Nakamura K, Ohta S, Ando H (2009) Therapeutic antitumor efficacy of monoclonal antibody against Claudin-4 for pancreatic and ovarian cancers. Cancer Sci 100: 1623–1630.

Tomita M, Hayashi M, Awazu S (1996) Absorption-enhancing mechanism of EDTA, caprate, and decanoylcarnitine in Caco-2 cells. J Pharm Sci 85: 608–611.

Tsukita S, Furuse M (1998) Overcoming barriers in the study of tight junction functions: from occludin to claudin. Genes Cells 3: 569–573.

Uchida H, Kondoh M, Hanada T, Takahashi A, Hamakubo T, Yagi K (2010) A claudin-4 modulator enhances the mucosal absorption of a biologically active peptide. Biochem Pharmacol 79: 1437–1444.

Biochemical and Biophysical Research Communications 410 (2011) 466–470

Contents lists available at ScienceDirect

Biochemical and Biophysical Research Communications

journal homepage: www.elsevier.com/locate/ybbrc

Mutated C-terminal fragments of *Clostridium perfringens* enterotoxin have increased affinity to claudin-4 and reversibly modulate tight junctions in vitro

Azusa Takahashi [a], Masuo Kondoh [a,*], Hiroshi Uchida [b], Yohei Kakamu [a], Takao Hamakubo [c], Kiyohito Yagi [a]

[a] *Laboratory of Bio-Functional Molecular Chemistry, Graduate School of Pharmaceutical Sciences, Osaka University, Osaka, Japan*
[b] *Asubio Pharma Co., Ltd., Kobe, Japan*
[c] *Department of Molecular Biology and Medicine, Research Center for Advanced Science and Technology, The University of Tokyo, Tokyo, Japan*

ARTICLE INFO

Article history:
Received 24 May 2011
Available online 6 June 2011

Keywords:
Tight junction
Claudin
Clostridium perfringens enterotoxin
Site-directed mutagenesis

ABSTRACT

Passage across epithelial cell sheets is the first step in drug absorption. Tight junctions (TJs) are located between adjacent epithelial cells and seal the intercellular space preventing leakage of solutes. Claudin, a tetra-transmembrane protein family, is a pivotal functional and structural component of the TJ barrier. Modulation of the claudin-based TJ seal is a strategy for mucosal drug absorption. We previously found that a claudin-4 binder, a C-terminal fragment of *Clostridium perfringens* enterotoxin (C-CPE194), was a modulator of the TJ seal and a potent mucosal absorption enhancer. In the present study, we attempted to improve claudin-4 binders by modification of C-CPE194. Substitution of Asn at position 309 and Ser at position 313 with Ala increased the affinity to claudin-4 by 9.9-fold as compared to C-CPE194. Deletion of 10 amino acids in the N-terminal domain of the double-alanine-substituted mutant increased affinity to claudin-4 by 23.9-fold as compared to C-CPE194. These C-CPE194 mutants reversibly modulated the TJ seal in human intestinal epithelial cell sheets. The N-terminal-truncated mutant was the most potent modulator of the TJ seal. These findings indicate that the C-CPE mutant may be a promising lead for the development of a clinical TJ modulator.

1. Introduction

Epithelium surrounds organisms and separates the inside of the body from the outside environment. Passage across the epithelium is the first step in drug absorption. Routes for solute movement across the epithelium are classified into transcellular and paracellular routes. Methods to deliver drugs through the transcellular route by simple diffusion or transporter- or receptor-mediated active transport have been developed since the 1990s, and some of these methods have been used clinically [1,2]. Absorption enhancers that deliver drugs through the paracellular route have been investigated since the 1960s, but most paracellular delivery systems have been investigated from the point of epithelial barrier-modulating activity [3,4]. Theoretical approaches for paracellular drug transport based on components of the epithelial barrier have never been fully developed because biochemical studies of the epithelial barrier have been sparse.

Tight junctions (TJs) are localized between adjacent epithelial cells and seal the intercellular space to prevent the leakage of solutes across the epithelial cell sheets. Modulation of the TJ barrier has been a strategy to enhance the epithelial absorption of drugs. However, biochemical and functional structures of TJs were not identified until 1998. Freeze-fracture replica electron microscopy analysis showed that TJs form a series of continuous, anastomotic and intramembranous particle strands, and the first structural and functional component of TJs, claudin, was identified in 1998 [5,6]. Claudin is a tetra-transmembrane protein with a molecular mass of ~23 kDa and comprises a family of 27 members [7,8]. Interestingly, the expression profiles and barrier functions of claudin family members differ among tissues. For instance, the epidermal barrier is disrupted in claudin-1-deficient mice, while the blood–brain barrier is deregulated in claudin-5-deficient mice [9,10]. These findings support the use of claudin-targeting strategies to enhance paracellular drug absorption.

Clostridium perfringens enterotoxin (CPE), a 35-kDa polypeptide, causes food poisoning in humans [11]. The CPE receptor is identical

Abbreviations: TJ, tight junction; C-CPE, the C-terminal fragment of *Clostridium perfringens* enterotoxin corresponding to 184-319 amino acids; CPE, *Clostridium perfringens* enterotoxin; DDM, *n*-dodecyl-β-D-maltoside; C-CPE194, C-terminal fragment of *Clostridium perfringens* enterotoxin corresponding to 194–319 amino acids; C-CPE205, C-terminal fragment of *Clostridium perfringens* enterotoxin corresponding to 205–319 amino acids; PCR, polymerase chain reaction; PBS, phosphate-buffered saline; SDS-PAGE, sodium dodecyl sulfate–polyacrylamide gel electrophoresis; BV, budded baculovirus; TBS, tris-buffered saline; ELISA, enzyme-linked immunosorbent assay; SPR, surface plasmon resonance; TEER, transepithelial electric resistance.

* Corresponding author. Fax: +81 6 6879 8199.
E-mail address: masuo@phs.osaka-u.ac.jp (M. Kondoh).

0006-291X/$ - see front matter © 2011 Elsevier Inc. All rights reserved.
doi:10.1016/j.bbrc.2011.05.161

to claudin-3 and -4, and the C-terminal fragment of CPE (C-CPE; amino acids 184–319) binds to claudin-3/-4 [12–15]. Interestingly, C-CPE reversibly modulates TJ seals in epithelial cell sheets [15]. We previously found that the jejunal absorption-enhancing activity of a claudin binder was 400-fold more potent than a clinically used absorption enhancer, sodium caprate, and that the claudin binder enhanced jejunal, pulmonary and nasal absorption of a biologically active peptide [16,17]. Thus, claudin binders are promising absorption enhancers, but claudin binders have never been fully developed because of the difficulty in preparation of the claudin proteins needed for screening claudin binders and the low antigenicity of claudin. To develop claudin binders using C-CPE as a prototype, we previously prepared alanine-substituted mutants and N-terminus-truncated mutants, and we investigated their claudin-4-binding and TJ-modulating activities [17–19]. Based on these findings on the functional domain of C-CPE, we modified C-CPE and prepared claudin-4 binders with higher affinity and TJ-modulating activity in the present study.

2. Materials and methods

2.1. Reagents

n-Dodecyl-β-D-maltoside (DDM) was purchased from Dojindo Laboratories (Kumamoto, Japan). Anti-claudin antibodies and anti-his-tag antibody were obtained from Invitrogen (Carlsbad, CA). CM5 sensor chips, amine-coupling reagents (*N*-ethyl-*N*′-(3-dimethylaminopropyl)-carbodiimide, *N*-hydroxysuccinimide, and ethanolamine–HCl) and HBS-EP+ (10 mM HEPES, pH 7.4, 150 mM NaCl, 3 mM EDTA and 0.05% surfactant P20) were obtained from GE Healthcare (Buckinghamshire, UK). All reagents used were of research grade.

2.2. C-CPE mutants

C-CPE is the first claudin binder to be identified [15]. N-terminal region-truncated C-CPE mutants are also claudin-4 binders: C-CPE194 (amino acids 194–319) and C-CPE205 (amino acids 205–319) [17,20]. The DNA fragment encoding alanine-substituted C-CPE194 or C-CPE205 was amplified by polymerase chain reaction (PCR) using the alanine-substituted primers and a template plasmid encoding C-CPE194 or C-CPE205, respectively [17]. The resulting PCR products were cloned into a pET16 vector. The plasmids were transduced into *E. coli* BL21 (DE3), and protein expression was stimulated by the addition of isopropyl-1-thio-β-D-galactoside. C-CPE mutants were purified from the cell lysates by affinity chromatography with HisTrap™ HP (GE Healthcare). The solvent was exchanged with phosphate-buffered saline (PBS) by gel filtration, and the purified proteins were stored at −80 °C until used. Purification of the proteins was confirmed by sodium dodecyl sulfate–polyacrylamide gel electrophoresis (SDS–PAGE) followed by staining with Coomassie Brilliant Blue. C-CPE mutants were quantified using a BCA protein assay kit with bovine serum albumin as a standard (Thermo Fisher Scientific Inc., Rockford, IL).

2.3. Claudin-displaying budded baculovirus (BV)

Claudin-displaying BV was prepared as described previously [21]. Claudin-1 and -4 cDNA fragments were cloned into the baculoviral transfer vector pFastBac1 (Invitrogen). Recombinant baculoviruses were generated using the Bac-to-Bac system according to the manufacturer's instructions (Invitrogen). Sf9 cells were cultured in Grace's Insect medium (Invitrogen) containing 10% fetal bovine serum at 27 °C and infected with the recombinant baculovirus. Seventy-two hours after infection, the BV fraction was isolated from the culture supernatant of the infected Sf9 cells by centrifugation at 40,000*g* for 25 min. The pellets of the BV fraction were suspended in Tris-buffered saline (TBS) containing protease inhibitor cocktail (Sigma–Aldrich, St. Louis) and then stored at 4 °C. The expression of claudins in the BV fraction was confirmed by SDS–PAGE and immunoblot with antibodies against claudins.

2.4. Enzyme-linked immunosorbent assay (ELISA)

The claudin-displaying BVs were adsorbed to the wells of 96-well immunoplates (Nunc, Roskilde, Denmark) overnight at 4 °C. The wells were blocked with 1.6% BlockAce (Dainippon Sumitomo Pharma, Osaka, Japan) for 2 h at room temperature. C-CPE mutants were added to the wells and incubated for an additional 2 h at room temperature. The wells were incubated with anti-his-tag antibody for 2 h at room temperature. The immunoreactive proteins were detected by a horseradish peroxidase-labeled secondary antibody with 3,3′,5,5′-tetramethylbenzine as a substrate. The reaction was terminated by the addition of 0.5 M H_2SO_4, and the immunoreactive proteins were measured at 450 nm.

2.5. Recombinant claudin-4 protein

Recombinant claudin-4 protein was prepared by an expression system using Sf9 cells and recombinant baculovirus as previously reported [17]. Briefly, the C-terminal his-tagged claudin-4 cDNA fragment was cloned into pFastBac1, and recombinant baculovirus was generated using the Bac-to-Bac baculovirus expression system. Sf9 cells were infected with the recombinant baculovirus. After 52–56 h of infection, the cells were harvested by centrifugation. The cells were resuspended in a solution of 10 mM HEPES (pH 7.4), 120 mM NaCl with protease inhibitors (Complete Mini, EDTA-free, Roche Applied Science), 1 mM phenylmethylsulfonyl fluoride and 20 U/ml DNase I. The cells were lysed with 2% DDM and then centrifuged. The resultant supernatant was applied to HisTrap™ HP, and claudin-4 was eluted with imidazole. The solvent for claudin-4 was changed to PBS containing 0.2% DDM by gel filtration with a HiTrap desalting column (GE Healthcare). Purification of claudin-4 was confirmed by SDS–PAGE followed by staining with Coomassie Brilliant Blue.

2.6. Surface plasmon resonance (SPR) analysis

SPR analysis was performed with a Biacore T100 instrument (GE Healthcare). Amine-coupling chemistry was used to immobilize claudin-4 at 25 °C on a CM5 sensor chip surface docked in a Biacore T100 and equilibrated with HBS-EP+. The carboxymethyl surface of the CM5 chip was activated for 2 min with a 1:1 ratio of 0.4 M *N*-ethyl-*N*′-(3-dimethylaminopropyl)-carbodiimide and 0.1 M *N*-hydroxysuccinimide at a flow rate of 10 μl/min. Claudin-4 was diluted to 2.5 μg/ml in 10 mM MES buffer (pH 6.5) and injected for 2 min over the surface at a flow rate of 10 μl/min. Excess activated groups were blocked by a 5-min injection of 1 M ethanolamine (pH 8.5) at a flow rate of 10 μl/min. Approximately 1000 RU of claudin-4 was immobilized using this protocol. Single-cycle kinetics experiments were performed at 25 °C with a flow rate of 30 μl/min [22]. C-CPE or its derivatives were serially diluted (1.25, 2.5, 5, 10 and 20 nM) in running buffer (HBS-EP+). Within a single binding cycle, samples of C-CPE or its derivatives were injected sequentially in order of increasing concentration over both the ligand and the reference surfaces. The reference surface, an unmodified flowcell, was used to correct for systematic noise and instrumental drift. Prior to the binding cycle for C-CPE or its derivatives, buffer was injected. These blank responses were used as a double-reference for the binding data [23]. The sensorgrams were globally fitted using a

1:1 binding model to determine k_a, k_d and K_D values with the Biacore T100 Evaluation Software version 2.0.1.

2.7. Transepithelial electric resistance (TEER) assay

Caco-2 cells were seeded onto Transwell™ chambers (Corning, NY) at a subconfluent density. The TEER of the Caco-2 monolayer cell sheets were monitored with a Millicell-ERS epithelial volt-ohmmeter (Millipore, Billerica, MA). When TJs were developed reaching a plateau in the TEER values, the cells were treated with C-CPEs on the basal side of the chambers. Changes in TEER values were monitored. The TEER values were normalized by the area of the Caco-2 monolayer cell sheets, and the TEER value of a blank chamber was subtracted. Relative TEER values were calculated by the ratio to TEER in the vehicle-treated chambers or before treatment.

3. Results

3.1. Preparation of C-CPE mutants

C-CPE is a 400-fold more potent mucosal absorption-enhancer than a clinically used absorption-enhancer, sodium caprate [16]. Partial N-terminal-deleted C-CPE derivatives, C-CPE194 and C-CPE205, had over 30- and 10-fold higher solubility in PBS than C-CPE without loss of binding to claudin-4, respectively [17]. An alanine-substitution analysis of C-CPE indicated that replacement of Asn at position 309 or Ser at position 313 by alanine may improve its binding to claudin-4 and modulation of the TJ barrier [18]. Based on these findings, we speculated that the combination of N-terminal deletion and alanine substitution may produce a potent claudin modulator. We first focused on C-CPE194 because it has the highest solubility. We prepared C-CPE194$_{N309A}$, C-CPE194$_{S313A}$ and C-CPE194$_{N309A/S313A}$ (Fig. 1). To determine if these C-CPE mutants could bind to claudin-4, we performed ELISA with claudin-4-displaying BV. As shown in Fig. 2, all of these C-CPE mutants dose-dependently bound to claudin-4-displaying BV but not wild-type BV. Next, we quantitatively investigated their affinity to claudin-4 by SPR analysis (Table 1). Substitution of Asn at position 309 did not affect affinity to claudin-4 (K_D values of C-CPE194, 455 pM; C-CPE194$_{N309A}$, 451 pM). Replacement of Ser at position 313 by alanine elevated affinity to claudin-4 (K_D value of C-CPE194$_{S313A}$, 117 pM). Interestingly, the double alanine-substituted C-CPE194$_{N309A/S313A}$ had synergistically higher affinity to claudin-4 (K_D value, 46 pM). Based on these results, we tested the affinity of C-CPE205 with replacements of both the Asn at position 309 and the Ser at position 313 by alanine (C-CPE205$_{N309A/S313A}$) (Fig. 1). The affinity of C-CPE205$_{N309A/S313A}$ to claudin-4 was the highest (K_D value, 19 pM) among the C-CPE mutants (Table 1).

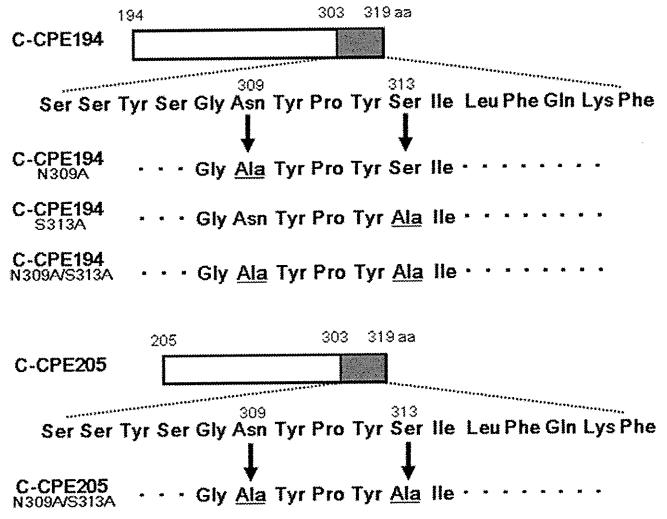

Fig. 1. Schematic illustration of C-CPE mutants. The C-terminal 16 amino acid fragment contains claudin-4-binding domains. A site-directed mutagenesis analysis of the C-terminal domain revealed that alanine substitution with Asn at position 309 or Ser at position 313 increased its binding to claudin-4 [18,19]. C-CPE194 and C-CPE205 are the C-terminal fragments of CPE corresponding to amino acids 194–319 and 205–319, respectively [17].

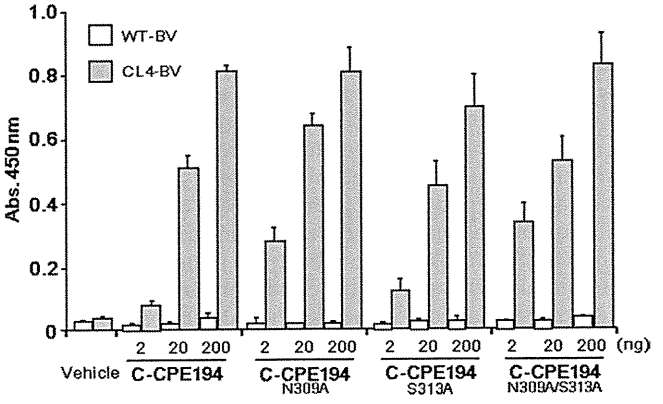

Fig. 2. Interaction of C-CPE mutants with claudin-4. Vehicle or C-CPE mutants were added to the wells of immunoplates coated with wild-type BV (WT-BV) or claudin-4-dysplaying BV (CL4-BV). After 2 h of incubation, anti-tag antibody, which recognized C-CPE mutants, was added to the wells, and then the C-CPE mutant-bound BV was detected by the addition of the horseradish peroxidase-labeled antibody, as described in Materials and methods. Data are representative of two independent experiments. The data are means ± SD ($n = 4$).

3.2. Effect of C-CPE mutants on the TJ seal

Next, we investigated the effects of C-CPE mutants on the modulation of the TJ seal. A monolayer culture of human colon Caco-2 cells is the most popular in vitro model for the assessment of TJ-seal modulation in the mucosal epithelium. As shown in Fig. 3A, treatment of monolayer cultures of Caco-2 cells with C-CPE mutants for 18 h dose-dependently decreased the integrity of TJ seals. The double alanine-substituted mutant C-CPE205$_{N309A/S313A}$ had the highest TJ-seal-modulating activity among the C-CPE mutants (CPE194: 62.7% and 31.7% of control at 5 and 20 μg/ml, respectively; C-CPE205$_{N309A/S313A}$: 14.6% and 10.3% of control at 5 and 20 μg/ml, respectively). The reversibility of TJ-seal modulation by a TJ modulator is important for safety. To investigate whether the C-CPE mutants reversibly modulated TJ integrity, C-CPE mutants were removed from the culture medium after 18 h, and then the cells were cultured for an additional 24 h. The TJ integrity was recovered 24 h after removal of the C-CPE mutants (Fig. 3B). These data indicate that the C-CPE mutants are reversible TJ modulators.

4. Discussion

Noninvasive drug administration is ideal for patient compliance and quality of life. Mucosal epithelium functions as a biological barrier preventing the free movement of solutes between the inside of the body and the outer environment. A strategy for noninvasive drug absorption is to modulate the TJ seal between adjacent mucosal epithelial cells. A C-terminal polypeptide fragment of CPE, referred to as C-CPE, modulates the TJ seal and binds to claudin-4 [15]. C-CPE enhanced the jejunal absorption of dextran by >400-fold as compared to a clinically used enhancer, and deletion of the claudin-4-binding domain attenuated its absorption-enhanc-

Table 1
Binding kinetics of C-CPE mutants to claudin-4.

Derivatives	ka(1/Ms)	kd (1/s)	K_D
C-CPE194	7.13×10^5	3.24×10^{-4}	455pM
C-CPE194$_{N309A}$	6.50×10^5	2.93×10^{-4}	451pM
C-CPE194$_{S313A}$	5.59×10^5	6.53×10^{-5}	117pM
C-CPE194$_{N309A/S313A}$	6.67×10^5	3.05×10^{-5}	46pM
C-CPE205$_{N309A/S313A}$	7.55×10^5	1.45×10^{-5}	19pM

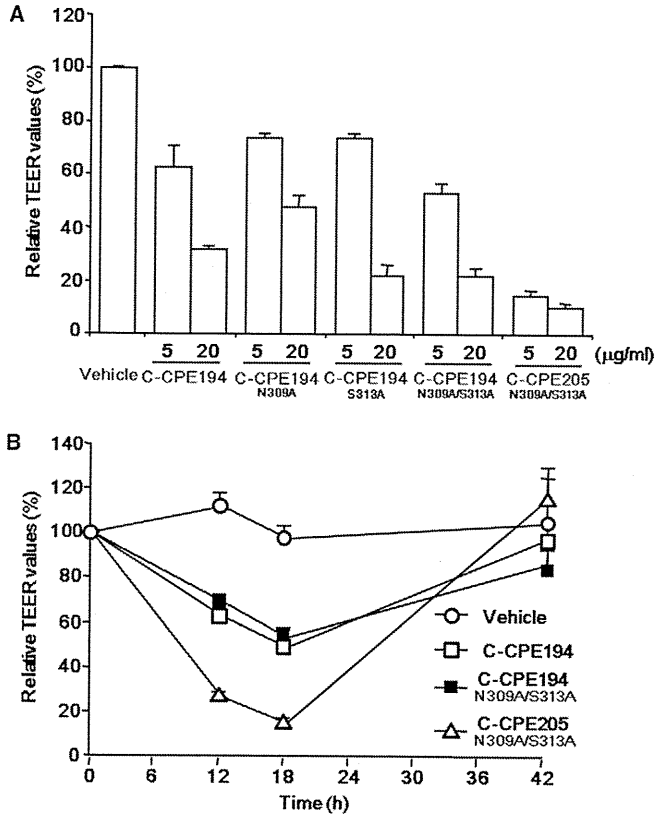

Fig. 3. Effect of C-CPE mutants on TJ-barrier in Caco-2 monolayer cell sheets. (A) Effect of C-CPE mutants on TJ-integrity. Caco-2 cells were cultured on Transwell™ inserts. When TEER values reached a plateau, the cells were treated with C-CPE or C-CPE mutants at 0, 5 or 20 μg/ml. After 18 h of C-CPE mutant treatment, the TEER values were monitored as described in the Materials and methods. The results were calculated as the percent of the TEER values to that of the vehicle-treated group. Data are representative of three independent experiments. The data are means ± SD ($n = 4$). (B) Reversibility of TJ modulation by C-CPE mutants. The cells were treated with C-CPE mutants (20 μg/ml) for 18 h, and then the cells were washed with the medium to remove the C-CPE mutants. The cells were cultured for an additional 24 h. Changes in TEER values were monitored during the C-CPE mutant treatment. The results were calculated as the percent of the TEER values to the values at 0 h. Data are representative of three independent experiments. The data are means ± SD ($n = 4$).

ing activity [16]. Claudin-4 binder may be useful for the development of a noninvasive drug delivery system. In the present study, we modified C-CPE based on our past functional domain mapping, and we found that the partial N-terminal-deleted and alanine-substituted mutants, C-CPE194$_{N309A/S313A}$ and C-CPE205$_{N309A/S313A}$, had higher affinity for claudin-4 and/or higher TJ-modulating activity than the parental C-CPE.

Why did substitution of Asn at position 309 and Ser at position 313 with Ala in C-CPE increase its affinity to claudin-4? Tyr residues at positions 306, 310 and 312 and Leu at position 315 in CPE are involved in the interaction between CPE and claudin-4 [18]. Winkler et al. proposed that C-CPE may interact with the hydrophobic turn in the second loop of claudin through its hydrophobic pit on the surface of C-CPE formed by those Tyr and Leu residues [24]. The substitution of Asn at position 309 and Ser at position 313 with Ala may reduce polarity and steric hindrance in the hydrophobic pit of C-CPE leading to increased binding of the Tyr and Leu residues to the hydrophobic region of claudin. Replacement of Ser at 305 or 307 by Ala also increased the binding of C-CPE to claudin-4 [18]. Tyr at position 306 is located between Ser residues at positions 305 and 307. Reduction of the polarity and steric hindrance surrounding Tyr at position 306, 310 and 312 and Leu at position 315 might increase the affinity of C-CPE to claudin-4.

C-CPE194$_{N309A/S313A}$ and C-CPE205$_{N309A/S313A}$ had 9.9- and 23.9-fold higher affinity to claudin-4 as compared to C-CPE194, respectively. However, their affinities to claudin-4 did not always affect their TJ-barrier-modulating activity. C-CPE205$_{N309A/S313A}$ modulated the TJ barrier more than C-CPE194, but C-CPE194$_{N309A/S313A}$ had TJ-barrier-modulating activity similar to C-CPE194. One possible explanation for this discrepancy may be differences in their cellular uptake activities. Claudin contains a clathrin-sorting signal in its C-terminal intracellular domain [25]. Treatment of cells with the C-terminal fragment of CPE caused a disappearance of claudin-4 in TJs and a decrease in claudin-4 protein [15]. Claudin-4 binders may first bind to claudin-4, after which the binders bound to claudin-4 may be taken up into the cytosol via endocytosis leading to the degradation of claudin-4. C-CPE205$_{N309A/S313A}$ might show higher endocytic activity by interacting with claudin-4 in a manner different than the other C-CPE mutants. These C-CPE mutants had similar association kinetics to claudin-4 but different dissociation kinetics to claudin-4 (Table 1). A longer interaction between C-CPE205$_{N309A/S313A}$ might increase the endocytosis of C-CPE mutant-bound claudin-4. Further experiments are needed to prove this hypothesis.

Preparation of antibodies against the extracellular domain of claudin-1, -3 and -4 has been recently reported [26–28]. However, to our knowledge, C-CPE is still the only modulator of the claudin barrier. C-CPE may be a promising lead for the development of TJ modulators. We have developed a screening system for claudin binders using a baculoviral display system [29]. We are attempting to develop novel claudin binders by the combination of a C-CPE mutant library and the baculoviral display system. Claudin-4-targeting is also a potent strategy for cancer-targeting and mucosal vaccination [21,27,30], for which C-CPE194$_{N309A/S313A}$ and C-CPE205$_{N309A/S313A}$ can be used. Taken together, our findings regarding C-CPE mutants will contribute to the development of not only drug-absorption enhancers but also claudin-targeted drug development, such as for cancer therapy and vaccines.

Acknowledgments

We thank all of the lab members for their useful comments and discussion, K. Takashiba (Asubio Pharma) and Y. Nakano (GE Healthcare) for their excellent technical assistance. We also thank Drs Y. Horiguchi (Osaka University) and M. Furuse (Kobe University) for providing us C-CPE cDNA and claudin cDNA, respectively. This work was supported by a Grant-in-Aid for Scientific Research from the Ministry of Education, Culture, Sports, Science and Technology, Japan (21689006), by a Health and Labor Sciences Research Grants from the Ministry of Health, Labor and Welfare of Japan, by Takeda Science Foundation, by Mochida Memorial Foundation for Medical and Pharmaceutical Research and by a Grant from Kansai Biomedical Cluster project in Saito, which is promoted by the Knowledge Cluster Initiative of the Ministry of Education, Culture, Sports, Science and Technology, Japan. A.T. is supported by Research Fellowships of the Japan Society for the Promotion of Science for Young Scientists.

References

[1] S. Majumdar, S. Duvvuri, A.K. Mitra, Membrane transporter/receptor-targeted prodrug design: strategies for human and veterinary drug development, Adv. Drug Deliv. Rev. 56 (2004) 1437–1452.

[2] N. Mizuno, T. Niwa, Y. Yotsumoto, Y. Sugiyama, Impact of drug transporter studies on drug discovery and development, Pharmacol. Rev. 55 (2003) 425–461.

[3] B.J. Aungst, Intestinal permeation enhancers, J. Pharm. Sci. 89 (2000) 429–442.

[4] E.S. Swenson, W.J. Curatolo, Intestinal permeability enhancement for proteins, peptides and other polar drugs: mechanisms and potential toxicity, Adv. Drug Delivery Rev. 8 (1992) 39–92.

[5] M. Furuse, K. Fujita, T. Hiiragi, K. Fujimoto, S. Tsukita, Claudin-1 and -2: novel integral membrane proteins localizing at tight junctions with no sequence similarity to occludin, J. Cell Biol. 141 (1998) 1539–1550.

[6] L.A. Staehelin, Further observations on the fine structure of freeze-cleaved tight junctions, J. Cell Sci. 13 (1973) 763–786.

[7] M. Furuse, S. Tsukita, Claudins in occluding junctions of humans and flies, Trends Cell Biol. 16 (2006) 181–188.

[8] K. Mineta, Y. Yamamoto, Y. Yamazaki, H. Tanaka, Y. Tada, K. Saito, A. Tamura, M. Igarashi, T. Endo, K. Takeuchi, S. Tsukita, Predicted expansion of the claudin multigene family, FEBS Lett. 585 (2011) 606–612.

[9] M. Furuse, M. Hata, K. Furuse, Y. Yoshida, A. Haratake, Y. Sugitani, T. Noda, A. Kubo, S. Tsukita, Claudin-based tight junctions are crucial for the mammalian epidermal barrier: a lesson from claudin-1-deficient mice, J. Cell Biol. 156 (2002) 1099–1111.

[10] T. Nitta, M. Hata, S. Gotoh, Y. Seo, H. Sasaki, N. Hashimoto, M. Furuse, S. Tsukita, Size-selective loosening of the blood–brain barrier in claudin-5-deficient mice, J. Cell Biol. 161 (2003) 653–660.

[11] B.A. McClane, G. Chakrabarti, New insights into the cytotoxic mechanisms of *Clostridium perfringens* enterotoxin, Anaerobe 10 (2004) 107–114.

[12] J. Katahira, N. Inoue, Y. Horiguchi, M. Matsuda, N. Sugimoto, Molecular cloning and functional characterization of the receptor for *Clostridium perfringens* enterotoxin, J. Cell Biol. 136 (1997) 1239–1247.

[13] J. Katahira, H. Sugiyama, N. Inoue, Y. Horiguchi, M. Matsuda, N. Sugimoto, *Clostridium perfringens* enterotoxin utilizes two structurally related membrane proteins as functional receptors in vivo, J. Biol. Chem. 272 (1997) 26652–26658.

[14] K. Morita, M. Furuse, K. Fujimoto, S. Tsukita, Claudin multigene family encoding four-transmembrane domain protein components of tight junction strands, Proc. Natl. Acad. Sci. USA 96 (1999) 511–516.

[15] N. Sonoda, M. Furuse, H. Sasaki, S. Yonemura, J. Katahira, Y. Horiguchi, S. Tsukita, *Clostridium perfringens* enterotoxin fragment removes specific claudins from tight junction strands: evidence for direct involvement of claudins in tight junction barrier, J. Cell Biol. 147 (1999) 195–204.

[16] M. Kondoh, A. Masuyama, A. Takahashi, N. Asano, H. Mizuguchi, N. Koizumi, M. Fujii, T. Hayakawa, Y. Horiguchi, Y. Watanbe, A novel strategy for the enhancement of drug absorption using a claudin modulator, Mol. Pharmacol. 67 (2005) 749–756.

[17] H. Uchida, M. Kondoh, T. Hanada, A. Takahashi, T. Hamakubo, K. Yagi, A claudin-4 modulator enhances the mucosal absorption of a biologically active peptide, Biochem. Pharmacol. 79 (2010) 1437–1444.

[18] A. Takahashi, E. Komiya, H. Kakutani, T. Yoshida, M. Fujii, Y. Horiguchi, H. Mizuguchi, Y. Tsutsumi, S. Tsunoda, N. Koizumi, K. Isoda, K. Yagi, Y. Watanabe, M. Kondoh, Domain mapping of a claudin-4 modulator, the C-terminal region of C-terminal fragment of *Clostridium perfringens* enterotoxin, by site-directed mutagenesis, Biochem. Pharmacol. 75 (2008) 1639–1648.

[19] A. Takahashi, M. Kondoh, A. Masuyama, M. Fujii, H. Mizuguchi, Y. Horiguchi, Y. Watanabe, Role of C-terminal regions of the C-terminal fragment of *Clostridium perfringens* enterotoxin in its interaction with claudin-4, J. Controlled Release 108 (2005) 56–62.

[20] C.M. Van Itallie, L. Betts, J.G. Smedley 3rd, B.A. McClane, J.M. Anderson, Structure of the claudin-binding domain of *Clostridium perfringens* enterotoxin, J. Biol. Chem. 283 (2008) 268–274.

[21] R. Saeki, M. Kondoh, H. Kakutani, S. Tsunoda, Y. Mochizuki, T. Hamakubo, Y. Tsutsumi, Y. Horiguchi, K. Yagi, A novel tumor-targeted therapy using a claudin-4-targeting molecule, Mol. Pharmacol. 76 (2009) 918–926.

[22] R. Karlsson, P.S. Katsamba, H. Nordin, E. Pol, D.G. Myszka, Analyzing a kinetic titration series using affinity biosensors, Anal. Biochem. 349 (2006) 136–147.

[23] D.G. Myszka, Improving biosensor analysis, J. Mol. Recognit. 12 (1999) 279–284.

[24] L. Winkler, C. Gehring, A. Wenzel, S.L. Muller, C. Piehl, G. Krause, I.E. Blasig, J. Piontek, Molecular determinants of the interaction between *Clostridium perfringens* enterotoxin fragments and claudin-3, J. Biol. Chem. 284 (2009) 18863–18872.

[25] A.I. Ivanov, A. Nusrat, C.A. Parkos, Endocytosis of epithelial apical junctional proteins by a clathrin-mediated pathway into a unique storage compartment, Mol. Biol. Cell 15 (2004) 176–188.

[26] I. Fofana, S.E. Krieger, F. Grunert, S. Glauben, F. Xiao, S. Fafi-Kremer, E. Soulier, C. Royer, C. Thumann, C.J. Mee, J.A. McKeating, T. Dragic, P. Pessaux, F. Stoll-Keller, C. Schuster, J. Thompson, T.F. Baumert, Monoclonal anti-claudin 1 antibodies prevent hepatitis C virus infection of primary human hepatocytes, Gastroenterology 139 (2010) 953–964.

[27] M. Kato-Nakano, M. Suzuki, S. Kawamoto, A. Furuya, S. Ohta, K. Nakamura, H. Ando, Characterization and evaluation of the antitumour activity of a dual-targeting monoclonal antibody against claudin-3 and claudin-4, Anticancer Res. 30 (2011) 4555–4562.

[28] M. Suzuki, M. Kato-Nakano, S. Kawamoto, A. Furuya, Y. Abe, H. Misaka, N. Kimoto, K. Nakamura, S. Ohta, H. Ando, Therapeutic antitumor efficacy of monoclonal antibody against Claudin-4 for pancreatic and ovarian cancers, Cancer Sci. 100 (2009) 1623–1630.

[29] H. Kakutani, A. Takahashi, M. Kondoh, Y. Saito, T. Yamaura, T. Sakihama, T. Hamakubo, K. Yagi, A novel screening system for claudin binder using baculoviral display, PLoS ONE 6 (2010) e16611.

[30] H. Kakutani, M. Kondoh, M. Fukasaka, H. Suzuki, T. Hamakubo, K. Yagi, Mucosal vaccination using claudin-4-targeting, Biomaterials 31 (2010) 5463–5471.

G Model
IJP-12173; No. of Pages 9
ARTICLE IN PRESS

International Journal of Pharmaceutics xxx (2011) xxx–xxx

Contents lists available at SciVerse ScienceDirect

International Journal of Pharmaceutics

journal homepage: www.elsevier.com/locate/ijpharm

A facile preparation method of a PFC-containing nano-sized emulsion for theranostics of solid tumors

Kouichi Shiraishi[a], Reiko Endoh[a], Hiroshi Furuhata[a], Masamichi Nishihara[b], Ryo Suzuki[c], Kazuo Maruyama[c], Yusuke Oda[c], Jun-ichiro Jo[d], Yasuhiko Tabata[d], Jun Yamamoto[e], Masayuki Yokoyama[a,*]

[a] Medical Engineering Laboratory, Research Center for Medical Science, The Jikei University School of Medicine, 3-25-8, Nishi-shinbashi, Minato-ku, Tokyo 105-8461, Japan
[b] International Institute for Carbon-Neutral Energy Research (I²CNER), Kyushu University, 744 Motooka, Nishi-ku, Fukuoka 819-0395, Japan
[c] Department of Biopharmaceutics, School of Pharmaceutical Sciences, Teikyo University, 1091-1 Suwarashi, Midori-ku, Sagamihara, Kanagawa 252-5195, Japan
[d] Department of Biomaterials, Institute for Frontier Medical Sciences, Kyoto University, 53 Kawara-cho Shogoin, Sakyo-ku, Kyoto 606-8507, Japan
[e] Division of Physics and Astronomy, Graduate School of Science, Kyoto University, Kitashirakawa Oiwake-cho, Sakyo-ku, Kyoto 606-8502, Japan

ARTICLE INFO

Article history:
Received 14 June 2011
Received in revised form 27 August 2011
Accepted 2 October 2011
Available online xxx

Keywords:
Theranostics
Tumor targeting
Ultrasound
Perfluorocarbon
Emulsion

ABSTRACT

Theranostics means a therapy conducted in a diagnosis-guided manner. For theranostics of solid tumors by means of ultrasound, we designed a nano-sized emulsion containing perfluoropentane (PFC5). This emulsion can be delivered into tumor tissues through the tumor vasculatures owing to its nano-size, and the emulsion is transformed into a micron-sized bubble upon sonication through phase transition of PFC5. The micron-sized bubbles can more efficiently absorb ultrasonic energy for better diagnostic images and can exhibit more efficient ultrasound-driven therapeutic effects than nano-sized bubbles. For more efficient tumor delivery, smaller size is preferable, yet the preparation of a smaller emulsion is technically more difficult. In this paper, we used a bath-type sonicator to successfully obtain small PFC5-containing emulsions in a diameter of ca. 200 nm. Additionally, we prepared these small emulsions at 40 °C, which is above the boiling temperature of PFC5. Accordingly, we succeeded in obtaining very small nano-emulsions for theranostics through a very facile method.

1. Introduction

'Theranostics', 'theranosis', or 'theragnosis' is a newly created term in the fields of imaging diagnosis and drug delivery systems. As a word, 'theranostics' (Chen, 2011; Lammers et al., 2010, 2011; MacKay and Li, 2010) is a combination of therapy and diagnosis, and is defined as therapy conducted in a diagnosis-guided manner. A typical example of theranostics is found in a carrier system containing both a contrast agent for diagnosis and a drug for therapy. Theranostics has been studied with various types of drug carriers including liposomes (Kamaly and Miller, 2010), small molecules (Kalber et al., 2011), nano-particles (Jeong et al., 2011; Kim et al., 2010), emulsions (Gianella et al., 2011), synthetic polymers (Bryson et al., 2009), polymeric micelles (Blanco et al., 2009; Kaida et al., 2010; Min et al., 2010; Nakamura et al., 2006; Shiraishi et al., 2009, 2010), and other nano-sized carrier systems (Ai, 2011; Moon et al., 2011; Pan et al., 2008; Sanson et al., 2011). Ultrasound is considered to be a preferable modality for theranostics because ultrasound has been well studied and developed for image diagnoses and local therapies such as ultrasound lithotresis and hyperthermia.

For theranostics of solid tumors, micron-sized bubbles (microbubbles) (Hernot and Klibanov, 2008; Schutt et al., 2003; Unger et al., 2004) have been actively studied because the bubbles provide strong contrasts in ultrasonic images, and because cavitation of microbubbles (Grishenkov et al., 2009) induced by ultrasound can effectively damage cells. Cells can be damaged by both jet-stream and heat that are generated in the bubbles' cavitation. In the design of microbubbles for tumor applications, the size of the microbubbles is a very important factor. Larger microbubbles can produce stronger ultrasound image contrasts. In contrast, smaller bubbles are preferred for efficient delivery into tumor tissues because the size of the trans-vascular passage from the bloodstream into the tumor interstitial space is of a diameter smaller than 1 μm. It is believed that the maximum diameter for efficient translocation into tumor tissues is 200–400 nm (Ishida et al., 1999; Litzinger et al., 1994; Nagayasu et al., 1996; Yuan et al., 1995). (In this diameter range, bubbles must be called nano-bubbles.) This is an essential dilemma concerning the size of bubbles used for

Abbreviations: PFC, perfluorocarbon; PFC5, perfluoropentane; PFC6, perfluorohexane; DBU, 1,8-diazabicyclo[5.4.0]undec-7-ene; PEG-P(Asp(C7F9)*x*), poly(ethylene glycol)-b-poly(4,4,5,5,6,6,7,7,7-nonafluoroheptyl aspartate) block copolymer.

* Corresponding author. Tel.: +81 3 3433 1111x2336; fax: +81 3 3459 6005.
E-mail address: masajun2093ryo@jikei.ac.jp (M. Yokoyama).

0378-5173/$ – see front matter © 2011 Elsevier B.V. All rights reserved.
doi:10.1016/j.ijpharm.2011.10.006

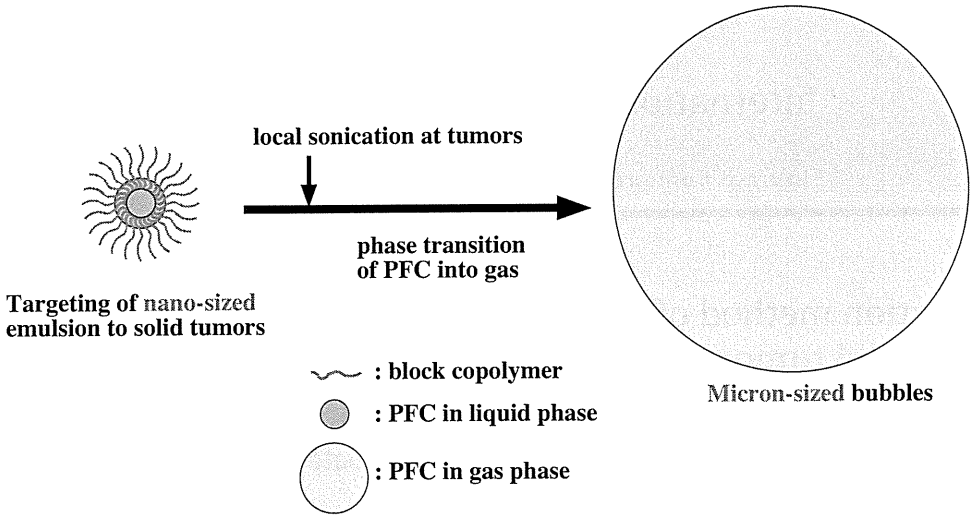

Fig. 1. Concept of phase-transition type nano-emulsion.

tumor theranostics. In order to resolve this dilemma, Kawabata et al. (Asami et al., 2009, 2010; Kawabata et al., 2005, 2010a,b) and Rapoport et al. (Mohan and Rapoport, 2010; Rapoport et al., 2007, 2009a, 2009b, 2010a,b, in press) examined nano-emulsions incorporating a specific kind of perfluorocarbon, as illustrated in Fig. 1. A boiling temperature of this perfluorocarbon (perfluoropentane, PFC5) is 29 °C, which is lower than normal human body temperature, but the integrity of these nano-emulsions is maintained owing to interfacial excessive pressure called Laplace pressure (Rapoport et al., 2009a). Upon ultrasound irradiation, the integrity of these nano-emulsions is broken, and this liquid perfluorocarbon exhibits a phase-transition into gas. Accordingly, the nano-emulsions change into microbubbles. Efficient delivery into tumor tissues is attained with the nano-emulsions, and then local sonication at the tumor tissues generates the microbubbles from the nano-emulsions, resulting in high imaging and therapeutic efficiencies. This phase-transition type nano-emulsion may be an ideal system for the theranostics of solid tumors.

Generally, preparations of smaller emulsions in a nano-meter range are more difficult because a higher power input is required in the emulsion preparations. (Tadros et al., 2004) Previously, we had prepared perfluorocarbon-containing emulsions by means of vigorous mechanical stirring with a magnetic stirrer and obtained emulsions of ca. 600 nm in diameter (Nishihara et al., 2009). In this paper, we have tried to obtain much smaller emulsions by means of ultrasound irradiation as well as high-pressure emulsification. Another important parameter for preparations of the phase-transition type nano-emulsion is temperature. A boiling temperature (29 °C) of perfluoropentane (PFC5) is close to the room temperature; therefore, preparations must be carried out at a low temperature and in a small scale for evasion of evaporation of PFC5 because heat generated in emulsification or sonication processes must be efficiently removed for the evasion. We want to find a facile preparation method that can be carried out at either room or a higher temperature, and that can be easily scaled up because the heat removal is a much less serious concern than the conventional method. Rapoport et al. (Rapoport et al., 2010b) reported preparations of nano-bubbles by means of ultrasound irradiation (with a probe type sonicator at 20 kHz) in ice-cold water. They obtained nano-emulsions of ca. 600 nm in diameter.

In this paper, we have tried to obtain very small nano-emulsions containing PFC5 by using an inexpensive bath-type sonicator (usually used as an ultrasonic cleaner) at room temperature or higher. For this emulsion preparation, we synthesized fluorinated block copolymers and optimized their compositions.

2. Materials and methods

2.1. Materials

We purchased perfluoropentane (PFC5) and perfluorohexane (PFC6) from Stream Chemicals (Newburyport, MA, USA) and Alfa Aesar (Ward Hill, MA, USA), respectively, and used them as received. We purchased 4,4,5,5,6,6,7,7,7-nonafluoroheptyl iodide from Sigma–Aldrich (Tokyo branch, Japan) and used it as received. We purchased reagent-grade solvents, dehydrated *N,N*-dimethylformamide (DMF), dimethyl sulfoxide (DMSO), and diethyl ether from Wako Chemicals (Tokyo, Japan), and used them as received. Poly(L-lactic acid)-grafted gelatin was prepared through a coupling reaction between a primary amine group of gelatin and a terminal hydroxyl group of the poly(L-lactic acid) by the use of disuccimidyl carbonate according to a published synthetic procedure. (Tanigo et al., 2010) Poly(ethylene glycol)-block-poly(L-lactic acid) block copolymer (PEG-b-PLA) was purchased from Sigma–Aldrich (Tokyo branch, Japan). The average molecular weights of the PEG block and the PLA block were 750 and 1,000, respectively.

2.2. Block copolymer synthesis

Poly(ethylene glycol)-*b*-poly(4,4,5,5,6,6,7,7,7-nonafluoroheptyl aspartate) block copolymers (PEG-P(Asp(C7F9)*x*)) were prepared by means of esterification of the aspartic units of poly(ethylene glycol)-b-poly(aspartic acid) block copolymer (PEG-P(Asp)) by the use of an iodinated compound, as shown in Fig. 2. PEG-P(Asp) was synthesized according to our previous paper (Yamamoto et al., 2007). A value *x* in the PEG-P(Asp(C7F9)*x*) formula denotes mol.% of the esterified units. This esterification reaction was carried out with a corresponding iodinated compound in the presence of a super base according to a previously reported procedure (Opanasopit et al., 2004; Yokoyama et al., 2004; Yamamoto et al., 2007) with a slight modification.

The starting material was poly(ethylene glycol)-b-poly(aspartic acid) block copolymer (PEG-P(Asp)). The average molecular weight of PEG was 5200 (n = 119 in Fig. 2), and the average number of Asp units per one chain was 26.0. The aspartate amide bond can be either α or β, and our group previously had reported that a ratio of α:β was 1:3 (=*a*:*b* in Fig. 2) (Yokoyama et al., 2004). PEG-P(Asp) (2.001 g, containing 6.33×10^{-3} mol Asp residue) was dissolved in 20 mL of DMF. To this mixture, was added both 4.904 g of 4,4,5,5,6,6,7,7,7-nonafluorohepty iodide (which is

Please cite this article in press as: Shiraishi, K., et al., A facile preparation method of a PFC-containing nano-sized emulsion for theranostics of solid tumors. Int J Pharmaceut (2011), doi:10.1016/j.ijpharm.2011.10.006

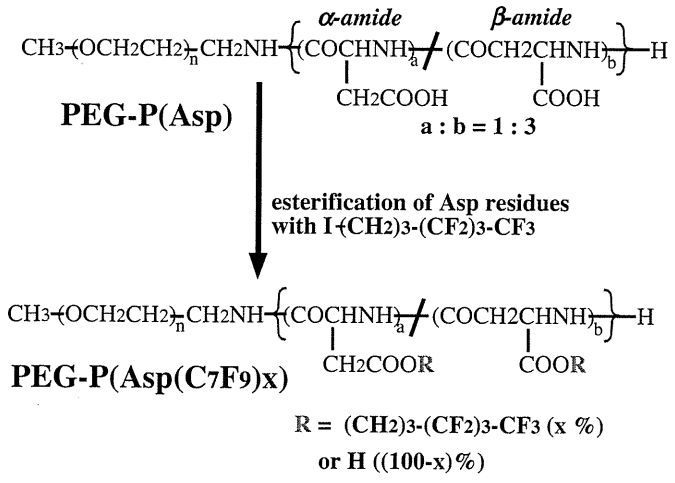

Fig. 2. Synthesis of the fluorocarbon-containing block copolymer PEG-P(Asp(C7F9)x).

2.00 mol. equivalents to the Asp residue, I-(CH2)3-(CF2)3-CF3 in Fig. 2) and 0.972 g of 1,8-diazabicyclo[5.4.0]undec-7-ene (DBU, which is 1.01 mol. equivalents to the Asp residue). DBU is a very strong base, and can induce ionization in a carboxyl group of the aspartic acid residue in an organic solvent, DMF. The reaction mixture was heated at 50 °C for 16 h. An ester formed at the Asp residue through a nucleophilic substitution reaction of the ionized carboxyl group with I-(CH2)3-(CF2)3-CF3. After this 16-h reaction, the reaction mixture was poured into 200 mL of ice-cold diethyl ether for precipitation of the polymer. The precipitated polymer was filtered and washed with diethyl ether. The obtained polymer was dissolved in 20 mL of DMSO, to which was added 2.11 mL of 6 N hydrochloric acid. This acid works for removal of DBU from polymers. This polymer solution was dialyzed with a Spectra/Por 6 dialysis membrane (molecular weight cut-off is 1000) against DMSO for 2 days and against milliQ water for an additional 2 days, followed by freeze-drying. Yield was 2.436 g. To determine the contents of the fluorinated ester group of the polymer, we used ^{1}H NMR spectroscopy in DMSO-d_6 containing 3 v/v% trifluoroacetic acid. For this determination, we identified a peak area ratio between the methylene protons ($-COOCH_2\underline{CH_2}CH_2CF_2CF_2CF_2CF_3$) at 1.8 ppm of the ester group and the methylene protons ($-OC\underline{H_2}C\underline{H_2}-$) at 3.6 ppm of the PEG block. The esterification percentage (x in Fig. 2) was revealed to be 59%. The other compositions of block copolymers were synthesized according to the same method with various molar ratios of I-(CH2)3-(CF2)3-CF3 and DBU with respect to the aspartic acid residue. Table 1 lists all the compositions of the synthesized block copolymers.

Table 1
Compositions of PEG-P(Asp(C7F9)x).

Code	M.W. of PEG	Asp unit number (n)	Esterification degree (x%)
F-6%	5200	22.1	5.9
F-15%	5200	23.3	14.6
F-39%	5200	22.1	38.5
F-59%	5200	26.0	58.5
F-67%	5200	22.1	67.0

2.3. Preparation of PFC-containing nano-emulsions

We examined preparations of PFC5-containing nano-emulsions according to two methods using a high-pressure emulsifier and a bath-type sonicator.

2.3.1. Preparation with a high-pressure emulsifier

We dissolved PEG-P(Asp(C7F9)15) block copolymer by stirring it in distilled water at a concentration of 4.0 wt. % of the solution, and added perfluoropentane (PFC5) and perfluorohexane (PFC6) at each 1.25 vol.% of the solution. We vigorously stirred the solution with a homogenizer Polytron (Kinematica AG, Tokyo, Japan) at 25,000 rpm for 10 s. Then, we conducted emulsification using a high-pressure emulsifier EmulsiFlex-C5 CSC (AVESTIN, Inc., Ottawa, Ontario, Canada) at 4 °C for 6 min at ca. 50 MPa. We collected a white emulsion, and filtered it with a Sartorius Minisart (R) filter (1.2 μm pore, Sartorius AG, Göttingen, Germany).

2.3.2. Preparation with a bath-type sonicator

We dissolved PEG-P(Asp(C7F9)x) block copolymers in MilliQ water at a concentration of 1.0 to 4.0 wt.% of water. In case of a high ester content such as x = 59, we heated (up to ca. 40 °C) and sonicated the solutions until we obtained a transparent polymer solution. The polymer solution was transferred to a 1.5-mL glass vial that was sealed with a Teflon–silicon rubber cap (Chromacol auto-sampler vial 2-SV for HPLC; GL Science, Inc., Tokyo, Japan), and was cooled on ice. Then, we added perfluoropentane (PFC5) and perfluorohexane (PFC6) at 0.5–4.0 vol.% of water. We confirmed PFCs' position at the bottom of the solution. (Sometimes PFCs, whose densities are much greater than water's, did not go into the aqueous solution. Therefore, we shook the vial vigorously to allow PFC droplets to sink to the bottom by force of gravity.) Then, we sealed the vial with a cap, and applied sonication for 3 min with a bath-type sonicator Branson model 1510 (oscillating frequency at 42 kHz, max. power intensity: 90 W, Danbury, CT, USA). The temperature of the bath was kept constant with degassed cold and hot water. In all the sonication procedures, we had a constant water level in a sonicator bath and a fixed position of the vial in order to obtain sonication conditions that were as identical to one another as possible. Finally, we collected a supernatant by leaving unincorporated PFC droplets at the bottom.

Table 2
Effects of polymer composition and sample volume on PFC5 incorporation behaviors.

Run	Polymer	Sample volume (μL)	PFC5 concentration (vol.%)[a]	Cumulant average diameter (nm)[a]
1	F-6%	300	0.840 ± 0.097	261.2 ± 3.4
2	F-15%	300	0.948 ± 0.131	232.4 ± 14.5
3	F-39%	300	0.625 ± 0.074	198.4 ± 33.3
4	F-59%	300	0.669[b]	133.9[b]
5	F-67%	300	0.682 ± 0.060	222.8 ± 37.9
6	F-59%	300	0.682 ± 0.074	205.5 ± 15.8
7	F-59%	300	0.634 ± 0.361	173.5 ± 24.5
8	F-59%	700	1.110[b]	231.8[b]
9	F-59%	1200	1.792[b]	280.6[b]

[a] Average ± standard deviation (n = 3) except runs 4, 8, and 9.
[b] Average of two preparations.

Please cite this article in press as: Shiraishi, K., et al., A facile preparation method of a PFC-containing nano-sized emulsion for theranostics of solid tumors. Int J Pharmaceut (2011), doi:10.1016/j.ijpharm.2011.10.006

In order to measure amounts of the polymer chains that were not included in the PFC-emulsions, we carried out the following experiment. PFC-emulsion was prepared in the conditions of Run 4 of Table 2; polymer: F-59%, sample volume: 300 μL, polymer concentration: 4 wt.%, PFC5: 2 vol.%, PFC6: 2 vol.%, sonication at 40 °C for 3 min. The obtained emulsion was transferred into a 1.5 mL Eppendorf-type poly(propylene) tube and centrifuged at 13,200 rpm for 5 min with an Eppendorf centrifuge model 5415D (Eppendorf Co., Ltd. Japan, Tokyo, Japan). The emulsion was found to precipitate at the bottom. 200 μL of the supernatant was collected and freeze-dried. We calculated the polymer amounts that were not included in the PFC-emulsions by multiplying 1.5 (=300 μL/200 μL) to the freeze-dried polymer weight. As a control, we carried out the same experiment just only for the polymer (without addition of TFC5 nor TFC6).

2.4. Measurements

2.4.1. Dynamic light scattering (DLS)

The size of emulsions was measured with a dynamic light scattering (DLS) instrument, the DLS-7000 (Otsuka Electronics, Tokyo, Japan). DLS samples were prepared through appropriate dilution of the emulsions with commercial distilled water for internal injection (Otsuka Pharmaceutical Co. Ltd., Tokyo, Japan). The measurements were made at 25 °C, and scattering was observed at a 90° angle with respect to the incident beam. The cumulant average particle size and the particle size distribution from a non-negative least square method were determined by the use of software provided with the instrument.

2.4.2. Gas chromatography

We measured concentrations of PFC5 using two gas chromatograph systems as described below. In both cases, we successfully obtained clear separation of PFC5's peak from PFC6's peak, and carried out quantitative analyses using a standard sample of PFC5. Therefore, the two gas chromatograph systems gave us identical results. However, we only used the (2) system described below for blood samples because its pre-heating function was essential for measurements of blood samples.

2.4.2.1. Gas chromatograph system. We measured PFC5 using a gas chromatograph model G-6000 (Hitachi High-Technologies Corporation, Tokyo, Japan) equipped with a Gaskuropack 54 80/100 packed column (GL Sciences, Inc., Tokyo, Japan) and an FID detector at 200 °C. Carrier gas was nitrogen at a flow rate of 300 mL/min. 5 μL of a sample solution were injected into the gas chromatograph system with a micro syringe at 0 min. Column temperature was controlled in the following manner; 100 °C (0 min), raised at a rate of 5 °C/min until 130 °C (6 min), and then raised at a rate of 60 °C/min until 190 °C (7 min), followed by maintenance of 190 °C for 2 min. PFC5 and PFC6 were found to elute at 3.8 min and 6.4 min, respectively.

2.4.2.2. Gas chromatograph system. We measured PFC5 using a gas chromatograph system GC-2014 (Shimadzu Corp., Kyoto, Japan) equipped with an FID detector at 250 °C. We used two tandem-connected two columns: DB-WAX 127-7012 (Agilent Technologies Japan, Ltd., Tokyo, Japan) and RESTEK Rt-QBond 19741 (Shimadzu GLC Ltd., Tokyo, Japan). Carrier gas was helium at a flow rate of 20 mL/min. Either 100 or 544 μL of a sample solution were heated at 200 °C and injected with a headspace autosampler TurboMatrix Trap 40 (PerkinElmer Japan Co., Ltd., Yokohama, Japan). Column temperature was constant at 150 °C. PFC5 and PFC6 were found to elute at 3.6 min and 4.4 min, respectively.

2.5. Measurements of PFC5 concentration in blood

In vivo PFC5 concentration profiles in blood were evaluated in Balb/c female mice (6 weeks old). 100 μL of PFC-emulsion was intravenously administered via lateral tail veins. The emulsions' PFC5 concentrations ranged from 0.429 to 0.670 vol.%. Blood (44 μL) was collected with a heparinized blood-collecting glass tube, and mixed with 500 μL of heparin solution in a capped sample tube of the (2) gas chromatograph system.

3. Results

3.1. General characteristics of the emulsion-preparation method with a bath-type sonicator

In representative conditions, we successfully obtained PFC5-containing nano-sized emulsions having diameters of ca. 200 nm in considerably high PFC5 yields. Fig. 3(a) and (b) shows diameter distributions measured by means of dynamic light scattering (DLS) for PEG-P(Asp(C7F9)59) (F-59% in Table 1). In these conditions, we dissolved 12.0 mg of polymer in 300 μL water (4.0 wt.% solution), and put this polymer solution in a 1.5 mL glass vial, followed by additions of 6 μL (corresponding to 2.0 vol.% of water) of PFC5 and 6 μL of PFC6. Sonication was performed for 3 min in a bath-type sonicator at 40 °C. In the first three preparations (run 6 in Table 2), the cumulant diameter obtained was 205.5 ± 15.8 nm (the average ± standard deviation; $n = 3$), and Fig. 3(a) shows the weight-weighted diameter distribution of one preparation. Almost uniformly distributed emulsions were obtained, and the diameter of the emulsion droplets had a very small size about 200 nm. In this run 6, PFC5 concentrations were 0.682 ± 0.074 vol.%. These values are considered large enough for ultrasound images (Kawabata et al., 2005, 2010a,b). In another set of three preparations (on another day, run 7 in Table 2), we obtained a very similar average diameter, 173.5 ± 24.5 nm (the average ± standard deviation; $n = 3$) and PFC5 concentrations. The diameter distribution of one preparation of run 7 is shown in Fig. 3(b). These two figures exhibited a major peak at about 200 nm, while a minor peak was seen in a larger diameter side and a smaller diameter side, as shown in Fig. 3(a) and (b), respectively. This difference may result from a slight variation in sonication conditions such as the position of samples and the water level of the sonicator. These emulsions were obtained and measured without any purification process after the sonication, and a large majority of the emulsions in weight were found to have a diameter of about 200 nm. All these results clearly indicate that this sonication method brought about very small nanometer-sized PFC5-containing emulsions with considerably high PFC5 concentrations.

We measured a proportion of polymer incorporated in the PFC-emulsion out of the feed polymer amount. In these preparation conditions (run 7 in Table 2), 75.4 ± 2.6% ($n = 3$) of the feed polymer was found in a supernatant obtained after centrifugation. (All the PFC-emulsions were observed to precipitate in this centrifugation.) When this measurement was carried out for the polymer alone, 93.8 ± 2.0% ($n = 3$) of the feed polymer was found in a supernatant obtained after centrifugation. Therefore, 18.4% (=93.8%–75.4%) of the feed polymer was considered to be incorporated into the PFC-emulsions. Removal of the free polymer chain, that was not incorporated into the PFC-emulsion, was not examined in this study. The removal is difficult because the free polymer existed as a polymeric micelle was close to the PFC-emulsion in size. (If the free polymer existed as a single polymer chain, a difference in size between the free polymer and the PFC-emulsion would be so large to allow separation such as ultrafiltration.)

Please cite this article in press as: Shiraishi, K., et al., A facile preparation method of a PFC-containing nano-sized emulsion for theranostics of solid tumors. Int J Pharmaceut (2011), doi:10.1016/j.ijpharm.2011.10.006

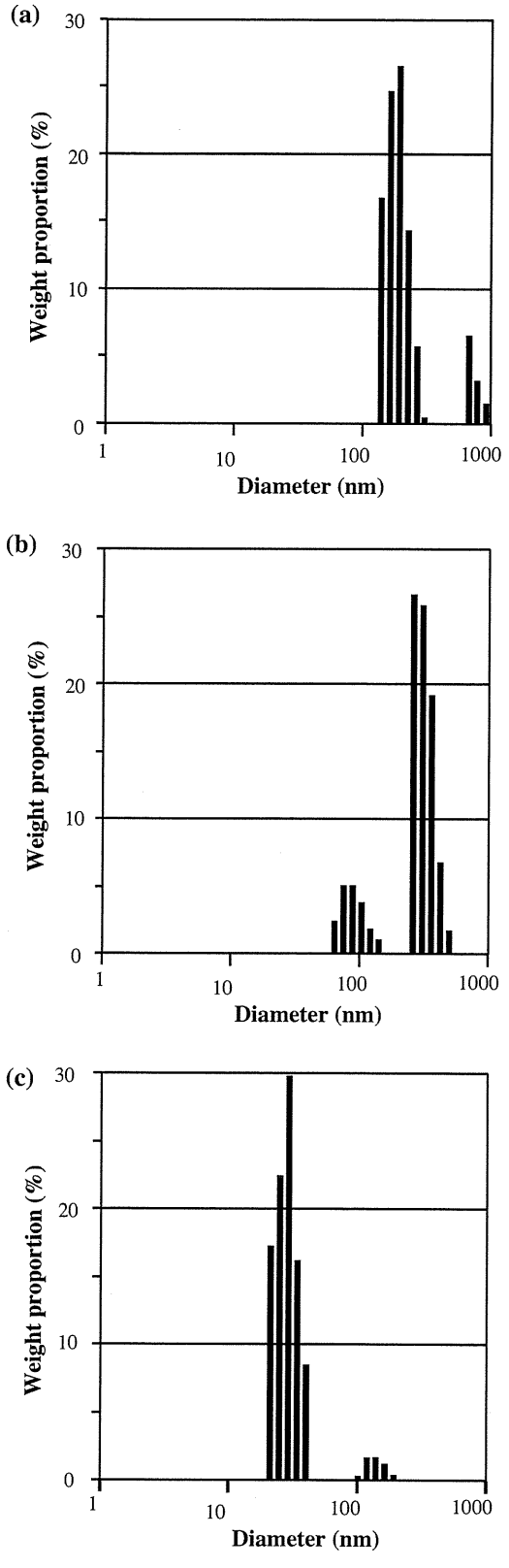

Fig. 3. Diameter distribution of PFC5-containing nano-emulsions (a and b) forming from PEG-P(Asp(C7F9)59) and empty polymeric micelle (c) measured by means of DLS. (a and b) are of different batches but prepared in the same conditions.

Using this polymer amount incorporated into the PFC-emulsions, we calculated the thickness of the polymer shell. We carried out the calculation with the following assumptions.

(1) The PFC-emulsions are made of the two phases; the inner PFC droplet phase and the outer polymer shell phase.
(2) We obtained PFC6 amounts in the emulsions assuming that sensitivity of PFC6 in gas chromatography is the same as that of PFC5. (The same peak area per PFC volume.)
(3) PFC6 and PFC5 are mixed freely without any gain or loss of droplet volume.
(4) Density of polymer is 1.03. (This is a common value of protein, and most synthetic polymers show similar values.)

The obtained value of the polymer shell's thickness was 22 nm, while the radius of the PFC droplet was 65 nm. In the future study, we like to analyse relationships between the shell thickness and physical stability of the emulsions.

3.2. Comparison with other emulsion-preparation methods

We compared the PFC5's concentrations of the PFC5-containing emulsions prepared in the sonication method with the PFC5's concentrations of the emulsions prepared in two common methods; mechanical stirring and high-pressure emulsification (Solans et al., 2005). We also compared the diameters of the emulsions prepared in the sonication method with those prepared in the two common methods. Previously, we reported PFC5-containing emulsions prepared by means of mechanical stirring that featured a magnetic stirrer (Nishihara et al., 2009). In this method, only the F-14% polymer provided a high PFC5 concentration (0.65 vol.%). The other polymers provided low or very low PFC5 concentrations: F-6% had 0.28 vol.%, F-22% had 0.19 vol.%, F-39% had 0.02 vol.%, and F-67% had 0.01 vol.%. In the F-14% case, the cumulant diameter was 694 nm, which was much larger than those obtained in the sonication method as described in the previous section (Section 3.1). Another distinct difference was found in a wide range of polymer compositions for high PFC5 concentrations in the sonication method. As summarized in runs 1–5 of Table 2, we compared the PFC5 concentrations (vol.%) and average diameters of the PFC5-containing emulsions for five polymer compositions. All these five compositions of polymers provided high PFC5 concentrations larger than 0.6 vol.%. Furthermore, all emulsion sizes of these runs (runs 2–5) were revealed to be small, at about 200 nm.

In the next step, we compared the sonication method with the most common method for emulsion preparation:high-pressure emulsification. For this comparison, we used F-15% polymer. We compared PFC5 concentrations and the cumulant average diameters of the emulsions prepared in the sonication method with PFC5 concentrations and the cumulant average diameters of the "high-pressure method" emulsions. We acquired a considerably high PFC5 concentration, 0.58 vol.%, by using a high-pressure emulsifier for the high-pressure emulsification method (its procedure is described in Section 2.3.1). However, the cumulant average diameter of the obtained emulsion was 477 nm. This value was much larger than the sonication-method value (232.4 nm, run 2 of Table 2). Additionally, maintenance of a low temperature at 4 °C for the whole instrument was essential in the high-pressure emulsification method, since possible heat generation due to the high-pressure process may considerably boost evaporation of PFC5 (the boiling temperature of PFC5 is 29 °C). In contrast, in the sonication method, a high PFC5 concentration was obtained at 40 °C, which is above PFC5's boiling temperature. (The temperature issue of the emulsion-preparation process will be more closely examined in the following section (Section 3.4).)

Please cite this article in press as: Shiraishi, K., et al., A facile preparation method of a PFC-containing nano-sized emulsion for theranostics of solid tumors. Int J Pharmaceut (2011), doi:10.1016/j.ijpharm.2011.10.006

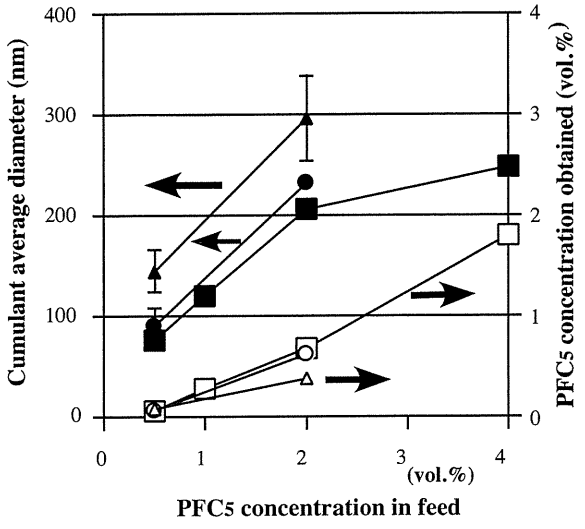

Fig. 4. Effects of polymer and PFC5 concentrations on physical properties of emulsions. PEG-P(Asp(C7F9)59) was used for emulsion preparations. Sample volume was 300 μL in 1.5-mL sample vials. Sonication was performed for 3 min at 40 °C. Filled plots represent cumulant average diameters, and vacant plots represent PFC5 concentrations of emulsions. Polymer concentration: △, ▲: 1.0 vol.%; ○, ●: 2.0 vol.%; □, ■: 4.0 vol.%.

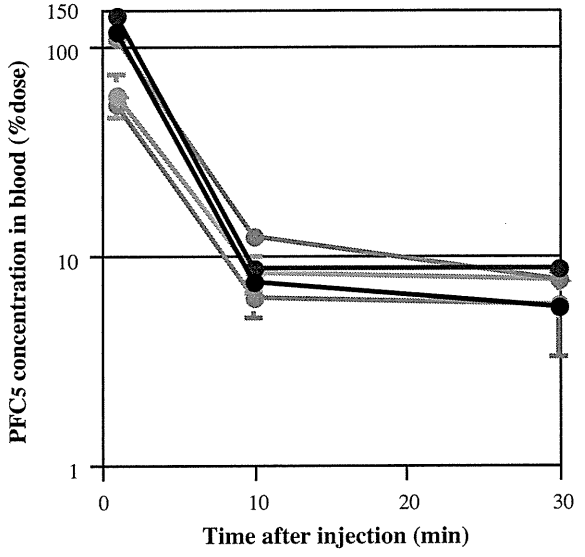

Fig. 5. Profiles of PFC5 concentration in blood. Black plot: run 1; blue plot: run 2; green plot: run 3; yellow plot: run 4; and red plot: run 5 (Table 5).

All these results indicate that the sonication method is a facile method for preparations of PFC5-containg emulsions with very small nano-sizes and high PFC5 concentrations.

3.3. Effects of sample volume, polymer concentration, and PFC5 concentration on incorporation behaviors

In the standard conditions, we put 300 μL water in a 1.5-mL of sealed glass tube and added polymer, PFC5, and PFC6. This configuration meant that a considerable amount of PFC5 perhaps would move from the solution into the glass tube's vacant atmospheric space (ca. 1.2 mL). We changed the volume of water while keeping constant the concentrations of polymer, PFC5, and PFC6 in the tube. Table 2 summarizes the results of runs 6–9 of Table 2. A higher PFC5 concentration was obtained in a case involving a larger water volume. (This means that there was a smaller vacant space in a sealed tube.) In accordance with the higher concentration of PFC5, the average diameter of the emulsion was observed to be larger. In run 9, PFC5's yield reached a very high value, approximately 90%. On the other hand, the PFC5's yield decreased to 32–33% when a small sample volume (300 μL) was adopted. These values indicate that the emulsification process can be well controlled through adjustment of sample volume.

Then, we examined effects that both polymer concentrations and PFC5 concentrations in feed had on the two physical values: diameter and PFC5 concentrations of the emulsion. Fig. 4 shows results of these two physical values for F-59% polymer cases. We changed the polymer concentration and the PFC5 concentration in feed in a range of 1.0–4.0 wt.% and of 0.5–4.0 vol.%, respectively. Each empty plot indicates PFC5 concentrations obtained for each polymer concentration, while each filled plot indicates cumulant average diameters for each polymer concentration. The polymer concentration was not found to significantly affect these two physical values. The polymer concentration affected very slightly the PFC5 content because three plot lines almost overlapped. When the polymer concentration was raised, only a small drop in the cumulant average diameter was observed. In contrast, the PFC5 concentration in feed was revealed to greatly affect the two physical values; larger values of PFC5 concentrations and cumulant average diameters were obtained with larger PFC5 concentrations in feed. Diameters of multi-modal distributions like Fig. 3(a) and (b) cannot be evaluated with the cumulant average diameters because the cumulant average diameters suppose the uni-modal diameter distribution. Therefore, we evaluated weight-weighted diameter distributions. Supplementary data, Table A summarizes and compares weight-weighted diameters with the cumulant average diameters. In most emulsion preparations, diameter distributions were found to be bi- or tri-modal, and therefore, exactly quantitative measurements of weight-weighted diameters are difficult in the homodyne analysis of dynamic light scattering done in this study. In fact, considerable differences are observed between the weight-weighted diameters and the cumulant average diameters for emulsions prepared in low PFC5 feed concentrations such as 1%, possibly due to the presence of empty polymeric micelles. (A DLS result of the empty micelle is shown in Fig. 3(c).) Even in this technical difficulty, the correlations obtained in Fig. 4a are not changed when multi-modal distributions are compared in the Supplementary data, Table A.

From the results obtained in this section, it was revealed that the sample volume and the PFC5 concentration in feed were appropriate factors for the facile control of size and the PFC5 content of the nano-sized emulsion.

3.4. Function of PFC6 in an emulsion preparation

In the above-described procedures for the emulsion preparation, we always used a 1:1 (vol./vol.) mixture of PFC5 and PFC6 in order to obtain a high PFC5 yield at a temperature higher than the boiling temperature of PFC5. We chose this 1:1 ratio because Kawabata et al. reported that ultrasound intensity required for the phase-transition (vaporization) induction at the 1:1 ratio was similar to that of a PFC5 alone case, and that this intensity was almost constant between ratios of 15:85, 50:50 (=1:1), and 85:15 (Asami et al., 2009). We varied temperatures (15, 25, 40, and 65 °C) of a sonicator's water bath, and performed the emulsion preparation both in the presence and the absence of PFC6 at each temperature. Table 3 summarizes results. In the absence of PFC6, PFC5 concentration was smaller than that of the corresponding PFC6-present case at every temperature. In runs 2 and 4, the obtained emulsions contained a considerable quantity of PFC5 over 0.2 vol.%. These two runs were prepared at lower temperatures than a boiling temperature of PFC5 (29 °C). Only a very small amount of PFC5

Please cite this article in press as: Shiraishi, K., et al., A facile preparation method of a PFC-containing nano-sized emulsion for theranostics of solid tumors. Int J Pharmaceut (2011), doi:10.1016/j.ijpharm.2011.10.006

Table 3
Effects of temperature and PFC6 addition on PFC5 incorporation behaviors.

Run	Temperature (°C)	PFC6 addition	PFC5 concentration (vol.%)[a]	Cumulant average diameter (nm)[a]
1	15	Yes	0.727 ± 0.191	210.8 ± 17.8
2	15	No	0.419 ± 0.124	82.7 ± 2.6
3	25	Yes	0.566 ± 0.367	177.1 ± 8.9
4	25	No	0.205 ± 0.086	95.7 ± 8.9
5[b]	40	Yes	0.634 ± 0.361	173.5 ± 24.5
6	40	No	0.049 ± 0.059	98.5 ± 5.1
7	65	Yes	0.154 ± 0.051	136.2 ± 16.0
8	65	No	0.096[c]	303.7[c]

[a] Average ± standard deviation ($n = 3$) except run 8.
[b] This run is identical to run 6 of Table 2.
[c] Average of two preparations.

was incorporated in run 6, which was performed at 40 °C, which is above PFC5's boiling temperature. This indicates that most PFC5 evaporated at 40 °C, and that interfacial Laplace pressure did not suppress PFC5's evaporation in the sonication procedure possibly because PFC5 evaporated from macroscopic PFC's droplets (in mm scale) before its incorporation into nano-emulsions where Laplace pressure's effect is great. In contrast, the PFC6-present cases presented similar amounts of PFC5 incorporated at 15, 25, and 40 °C. This means that PFC5's evaporation at 40 °C was efficiently suppressed through the mixing with PFC6. PFC5 and PFC6 not only are miscible but also these two compounds are expected to strongly interact with each other because these are both perfluorocarbons. It is considered that PFC5 evades evaporation through the strong interaction with PFC6 that has a higher boiling temperature than 40 °C. In run 7, performed at 65 °C, a considerable drop in the incorporated PFC5 amount was seen. This sonication temperature (65 °C) is higher than PFC6's boiling temperature (60 °C), and therefore, both PFC5 and PFC6 were evaporated at 65 °C. From these results, we have confirmed the function of the added PFC6 for high PFC5-incorporation amounts at a temperature higher than PFC5's boiling temperature.

3.5. PFC5 concentration profile in blood

We measured PFC concentrations in blood using several PFC5-containing emulsions in order to control their pharmacokinetic behaviors. For a larger amount of emulsion accumulation at tumor tissues, a longer half-life is preferable for a contrast agent. In contrast, a shorter half-life is advantageous for a diagnosis in a short period after injection of a contrast injection, since a low concentration of the contrast agent in blood is a pre-requisite for a high contrast image of the contrast agent's accumulated region. Under this contradictory situation for the optimum half-life, it is very important to obtain technologies to control (prolong and shorten) a half-life of the contrast agent.

We used three different types of polymers including PEG-P(Asp(C7F9)x) block copolymers in order to control half-livers in blood. In Table 4, we describe the compositions of the two copolymers other than PEG-P(Asp(C7F9)x). These two copolymers contain hydrophobic poly(L-lactic acid) chains that are expected to work for incorporation of hydrophobic PFC5 into emulsions. Table 5 summarizes five samples prepared from four polymers. By adjusting the vacant volume of a 1.5-mL glass vial to a small value (ca., 300 μL, meaning 1.2 mL of the sample volume.), we successfully obtained emulsions with higher PFC5 contents than 0.4 vol.% in runs 1–3. In these cases, the sonication was carried out at 15 °C. When emulsions were prepared in the same conditions of run 1 except for a different temperature (at 40 °C) and a different vacant volume (ca. 0 μL), the PFC5 content was considerably lower (0.408 vol.%) than in run 1.

Table 4
Compositions of two poly(L-lactic acid)(PLA)-containing polymers.

Code	Structure	Compositions
Gelatin derivative	Poly(L-lactic acid)-grafted gelatin	M.W. of PLA: 1000 weight ratio PLA/gelatin = 0.17
PEG-PLA	Poly(ethylene glycol)-b-Poly(L-lactic acid) Block copolymer	M.W. of PEG: 2000 M.W. of PLA: 1000

We injected these five samples in a mouse tail vein. As shown in Fig. 5, we observed a distinct difference in PFC5 concentrations at 1 min after the injection between three runs containing PLA (runs 1–3) and the other two runs for PEG-P(Asp(C7F9)x). The former three runs showed almost a 100% dose at 1 min with an assumption that blood volume was 7 vol./wt.% of body weight, while the latter two runs provided considerably smaller values than the 100% dose. In all runs, however, PFC5 concentrations were rapidly lowered at 10 and 30 min after the injection, and no clear difference was observed at these time points among all the runs. Therefore, control of pharmacokinetic behaviors, in particular prolongation of blood half-life from a few minutes, was not successfully achieved in this examination by the use of different polymer structures. For the pharmacokinetic control of the emulsions, an additional functional component may be required. Rapoport et al. (Rapoport et al., 2011) reported a very stable circulation (half-life = 2–4 h) in blood for perfluoro-crown-ether compound containing nano-emulsions.

Table 5
Compositions of PFC-emulsions for in vivo experiments.

Run	Polymer	Polymer concentration in feed (%)[a]	PFC5 concentration in feed (vol.%)	PFC5 concentration obtained in emulsion (vol.%)	Cumulant average diameter (nm)
1	Gelatin derivative[b]	1.0	1.25[d]	0.613	345.9
2	Gelatin derivative[b]	4.0	1.25[d]	0.429	542.6
3	PEG-b-PLA[a]	4.0	1.0[d]	0.491	222.6
4	F-15%[c]	4.0	2.0	0.465	256.3
5	F-59%[c]	4.0	1.0	0.670	225.1

[a] Weight (g)/water volume (mL).
[b] Listed in Table 4.
[c] Listed in Table 1.
[d] Sonication at 15 °C.

Please cite this article in press as: Shiraishi, K., et al., A facile preparation method of a PFC-containing nano-sized emulsion for theranostics of solid tumors. Int J Pharmaceut (2011), doi:10.1016/j.ijpharm.2011.10.006

According to this report, a perfluoro compound showing stable emulsion formation may be utilized for stable incorporation of another PFC.

4. Discussion

In the examinations of this study, we successfully obtained very small (ca. 200 nm in diameter) PFC5-containing emulsions with high PFC5 contents in a very facile method using a common bath-type sonicator. Actually, the used sonicator was the smallest model with the lowest sonication power (max. Input power: 90 W) in its product line. The other facile aspect of this preparation method is the working temperature. By mixing PFC6 we performed the emulsion preparation at 40 °C, which is above the boiling temperature of PFC5. In a conventional method's use of a high-pressure emulsifier, cooling of the whole system is required for evading a large amount evaporation of PFC5 due to heat generated within a high-pressure emulsifier. In contrast, we did not need cooling samples during the preparation. This facileness is substantially important when we consider a scale-up of the emulsion preparations. In a large-scale production of these emulsions, the heat generated in preparation processes (both in emulsification and sonication) may become large enough to raise a temperature of the solution above the boiling temperature. Therefore, successful preparations at a high temperature means that there is a large margin for large-scale preparation with high PFC5 content as well as easy handling of samples at room temperature throughout the sonication procedure.

We could not substantially change pharmacokinetic behaviors of the PFC5-containing emulsion, even when using different polymers. This is a very different situation from polymeric micelle drug carrier cases where block polymer structure was revealed to be a very influential factor on pharmacokinetic behaviors of the incorporated drug into the polymeric micelles (Yokoyama, 2005, 2007; Watanabe et al., 2006). This difference may result from the liquid state of the emulsion's core, while the solid core is essential for stable drug incorporation in the polymeric micelle systems. An alternative and novel method may be required to obtain stable incorporation of liquid PFC for dramatically changed pharmacokinetics.

5. Conclusion

By using a bath-type sonicator, we successfully obtained PFC5-containing emulsions in a diameter range of 200 nm. These emulsions are very potent for theranostics of solid tumors through ultrasound irradiation. Furthermore, these emulsions were prepared in high PFC5 yields at 40 °C, which is higher than the boiling temperature of PFC5. This very facile preparation method is an important technological key for large-scale production of these medically valuable emulsions.

Acknowledgements

This work was supported by the New Energy and Industrial Technology Development Organization, Japan. M. Yokoyama, K. Shiraishi, and M. Nishihara acknowledge support from the JST CREST program, Grant-in-Aid of the Ministry of Education, Culture, Sports, Science and Technology, Japan, and Kanagawa Academy of Science and Technology. The authors acknowledge Dr. Kenichi Kawabata and Dr. Rei Asami of Central Research Laboratory, Hitachi, Ltd., for their valuable discussion on PFC-containing nanoemulsions.

Appendix A. Supplementary data

Supplementary data associated with this article can be found, in the online version, at doi:10.1016/j.ijpharm.2011.10.006.

References

Ai, H., 2011. Layer-by-layer capsules for magnetic resonance imaging and drug delivery. Adv. Drug Deliv. Rev. 63, 772–788.
Asami, R., Azuma, T., Kawabata, K., 2009. Fluorocarbon droplets as next generation contrast agents—their behavior under 1–3 mhz ultrasound. IEEE Proc. Int. Ultrasonics Symp., 1294–1297.
Asami, R., Ikeda, T., Azuma, T., Kawabata, K., Umemura, S., 2010. Acoustic signal characterization of phase change nanodroplets in tissue-mimicking phantom gels. Jpn. J. Appl. Phys. 49, 07HF16.
Blanco, E., Kessinger, C.W., Sumer, B.D., Gao, J., 2009. Multifunctional micellar nanomedicine for cancer therapy. Exp. Biol. Med. 234, 123–131.
Bryson, J.M., Fichter, K.M., Chu, W.J., Lee, J.H., Li, J., Madsen, L.A., McLendon, P.M., Reineke, T.M., 2009. Polymer beacons for luminescence and magnetic resonance imaging of DNA delivery. Proc. Natl. Acad. Sci. U.S.A. 106, 16913–16918.
Chen, X.S., 2011. Introducing theranostics journal—from the editor-in-chief. Theranostics 1, 1–2.
Gianella, A., Jarzyna, P.A., Mani, V., Ramachandran, S., Calcagno, C., Tang, J., Kann, B., Dijk, W.J., Thijssen, V.L., Griffioen, A.W., Storm, G., Fayad, Z.A., Mulder, W.J., 2011. A multifunctional nanoemulsion platform for imaging guided therapy evaluated in experimental cancer. ACS Nano 5, 4422–4433.
Grishenkov, D., Pecorari, C., Brismar, T.B., Paradossi, G., 2009. Characterization of acoustic properties of PVA-shelled ultrasound contrast agents: ultrasound-induced fracture (part II). Ultrasound Med. Biol. 35, 1139–1147.
Hernot, S., Klibanov, A.L., 2008. Microbubbles in ultrasound-triggered drug and gene delivery. Adv. Drug Deliv. Rev. 60, 1153–1166.
Ishida, O., Maruyama, K., Sasaki, K., Iwatsuru, M., 1999. Size-dependent extravasation and interstitial localization of polyethyleneglycol liposomes in solid tumor-bearing mice. Int. J. Pharm. 190, 49–56.
Jeong, H., Huh, M., Lee, S.J., Koo, H., Kwon, I.C., Jeong, S.Y., Kim, K., 2011. Photosensitizer-conjugated human serum albumin nanoparticles for effective photodynamic therapy. Theranostics 1, 230–239.
Kaida, S., Cabral, H., Kumagai, M., Kishimura, A., Terada, Y., Sekino, M., Aoki, I., Nishiyama, N., Tani, T., Kataoka, K., 2010. Visible drug delivery by supramolecular nanocarriers directing to single-platformed diagnosis and therapy of pancreatic tumor model. Cancer Res. 70, 7031–7041.
Kalber, T.L., Kamaly, N., Higham, S.A., Pugh, J.A., Bunch, J., McLeod, C.W., Miller, A.D., Bell, J.D., 2011. Synthesis and characterization of a theranostic vascular disrupting agent for in vivo MR imaging. Bioconjug. Chem. 22, 879–886.
Kamaly, N., Miller, A.D., 2010. Paramagnetic liposome nanoparticles for cellular and tumour imaging. Int. J. Mol. Sci. 11, 1759–1776.
Kawabata, K., Sugita, N., Yoshikawa, H., Azuma, T., Umemura, S., 2005. Nanoparticles with multiple perfluorocarbons for controllable ultrasonically induced phase shifting. Jpn. J. Appl. Phys. 44, 4548–4552.
Kawabata, K., Asami, R., Yoshikawa, H., Azuma, T., Umemura, S., 2010a. Acoustic response of microbubbles derived from phase-change nanodroplet. Jpn. J. Appl. Phys. 49, 07HF18.
Kawabata, K., Asami, R., Yoshikawa, H., Azuma, T., Umemura, S., 2010b. Sustaining microbubbles derived from phase change nanodroplet by low-amplitude ultrasound exposure. Jpn. J. Appl. Phys. 49, 07HF20.
Kim, K., Kim, J.H., Park, H., Kim, Y.S., Park, K., Nam, H., Lee, S., Park, J.H., Park, R.W., Kim, I.S., Choi, K., Kim, S.Y., Park, K., Kwon, I.C., 2010. Tumor-homing multifunctional nanoparticles for cancer theragnosis: simultaneous diagnosis, drug delivery, and therapeutic monitoring. J. Contr. Rel. 146, 219–227.
Lammers, T., Kiessling, F., Hennink, W.E., Storm, G., 2010. Nanotheranostics and image-guided drug delivery: current concepts and future directions. Mol. Pharm. 7, 1899–1912.
Lammers, T., Aime, S., Hennink, W.E., Storm, G., Kiessling, F., 2011. Theranostic Nanomedicines. Acc. Chem. Res. 44, 1029–1038.
Litzinger, D.C., Buiting, A.M.J., van Rooijen, N., Huang, L., 1994. Effect of liposome size on the circulation time and intraorgan distribution of amphipathic poly(ethylene glycol)-containing liposomes. Biochim. Biophys. Acta 1190, 99–107.
MacKay, J.A., Li, Z., 2010. Theranostic agents that co-deliver therapeutic and imaging agents? Adv. Drug Deliv. Rev. 62, 1003–1004.
Min, K.H., Kim, J.H., Bae, S.M., Shin, H., Kim, M.S., Park, S., Lee, H., Park, R.W., Kim, I.S., Kim, K., Kwon, I.C., Jeong, S.Y., Lee, D.S., 2010. Tumoral acidic pH-responsive MPEG-poly(beta-amino ester) polymeric micelles for cancer targeting therapy. J. Contr. Rel. 144, 259–266.
Mohan, P., Rapoport, N., 2010. Doxorubicin as a molecular nanotheranostic agent: effect of doxorubicin encapsulation in micelles or nanoemulsions on the ultrasound-mediated intracellular delivery and nuclear trafficking. Mol. Pharm. 6, 1959–1973.
Moon, G.D., Choi, S.W., Cai, X., Li, W., Cho, E.C., Jeong, U., Wang, L.V., Xia, Y., 2011. A new theranostic system based on gold nanocages and phase-change materials with unique features for photoacoustic imaging and controlled release. J. Am. Chem. Soc. 133, 4762–4765.
Nagayasu, A., Uchiyama, K., Nishida, T., Yamagiwa, Y., Kawai, Y., Kiwada, H., 1996. Is control of distribution of liposomes between tumors and bone marrow possible? Biochim. Biophys. Acta 1278, 29–34.
Nakamura, E., Makino, K., Okano, T., Yamamoto, T., Yokoyama, M., 2006. A polymeric micelle MRI contrast agent with changeable relaxivity. J. Contr. Rel. 114, 325–333.
Nishihara, M., Imai, K., Yokoyama, M., 2009. Preparation of perfluorocarbon/fluoroalkyl polymer nanodroplets for cancer-targeted ultrasound contrast agents. Chem. Lett. 38, 556–557.

Please cite this article in press as: Shiraishi, K., et al., A facile preparation method of a PFC-containing nano-sized emulsion for theranostics of solid tumors. Int J Pharmaceut (2011), doi:10.1016/j.ijpharm.2011.10.006

Opanasopit, P., Yokoyama, M., Watanabe, M., Kawano, K., Maitani, Y., Okano, T., 2004. Block copolymer design for camptothecin incorporation into polymeric micelles for passive tumor targeting. Pharm. Res. 21, 2003–2010.
Pan, D., Caruthers, S.D., Hu, G., Senpan, A., Scott, M.J., Gaffney, P.J., Wickline, S.A., Lanza, G.M., 2008. Ligand-directed nanobialys as theranostic agent for drug delivery and manganese-based magnetic resonance imaging of vascular targets. J. Am. Chem. Soc. 130, 9186–9187.
Rapoport, N., Gao, Z., Kennedy, A., 2007. Multifunctional nanoparticles for combining ultrasonic tumor imaging and targeted chemotherapy. J. Natl. Cancer Inst. 99, 1095–1106.
Rapoport, N.Y., Kennedy, A.M., Shea, J.E., Scaife, C.L., Nam, K.H., 2009a. Controlled and targeted tumor chemotherapy by ultrasound-activated nanoemulsions/microbubbles. J. Contr. Rel. 138, 268–276.
Rapoport, N.Y., Nam, K.H., Gao, Z., Kennedy, A., 2009b. Application of ultrasound for targeted nanotherapy of malignant tumors. Acoust. Phys. 55, 594–601.
Rapoport, N., Christensen, D.A., Kennedy, A.M., Nam, K.H., 2010a. Cavitation properties of block copolymer stabilized phase-shift nanoemulsions used as drug carriers. Ultrasound Med. Biol. 36, 419–429.
Rapoport, N., Kennedy, A.M., Shea, J.E., Scaife, C.L., Nam, K.H., 2010b. Ultrasonic nanotherapy of pancreatic cancer: lessons from ultrasound imaging. Mol. Pharm. 7, 22–31.
Rapoport, N., Nam, K.H., Gupta, R., Gao, Z., Mohan, P., Payne, A., Todd, N., Liu, X., Kim, T., Shea, J., Scaife, C., Parker, D.L., Jeong, E.K., Kennedy, A.M., 2011. Ultrasound-mediated tumor imaging and nanotherapy using drug loaded, block copolymer stabilized perfluorocarbon nanoemulsions. J. Contr. Rel. 153, 4–15.
Sanson, C., Diou, O., Thévenot, J., Ibarboure, E., Soum, A., Brûlet, A., Miraux, S., Thiaudière, E., Tan, S., Brisson, A., Dupuis, V., Sandre, O., Lecommandoux, S., 2011. Doxorubicin loaded magnetic polymersomes: theranostic nanocarriers for MR imaging and magneto-chemotherapy. ACS Nano 5, 1122–1140.
Schutt, E.G., Klein, D.H., Mattrey, R.M., Riess, J.G., 2003. Injectable microbubbles as contrast agents for diagnostic ultrasound imaging: the key role of perfluorochemicals. Angew. Chem. Int. Ed. Engl. 42, 3218–3235.
Shiraishi, K., Kawano, K., Minowa, T., Maitani, Y., Yokoyama, M., 2009. Preparation and in vivo imaging of PEG-poly(L-lysine)-based polymeric micelle MRI contrast agents. J. Contr. Rel. 136, 14–20.
Shiraishi, K., Kawano, K., Maitani, Y., Yokoyama, M., 2010. Synthesis of Poly(ethylene glycol)-b-poly(L-lysine) block copolymers having Gd-DOTA as MRI contrast agent and their polymeric micelle formation by polyion complexation. J. Contr. Rel. 148, 160–167.
Solans, C., Izquierdo, P., Nolla, J., Azemar, N., Garcia-Celma, M.J., 2005. Nano-emulsions. Curr. Opin. Colloid Interface Sci. 10, 102–110.
Tadros, T., Izuquierdo, P., Esquena, J., Solans, C., 2004. Formation and stability of nano-emulsions. Adv. Colloid Interface. Sci. 108–109, 303–318.
Tanigo, T., Takaoka, R., Tabata, Y., 2010. Sustained release of water-insoluble simvastatin from biodegradable hydrogel augments bone regeneration. J. Contr. Rel. 143, 201–206.
Unger, E.C., Porter, T., Culp, W., Labell, R., Matsunaga, T., Zutshi, R., 2004. Therapeutic applications of lipid-coated microbubbles. Adv. Drug Deliv. Rev. 56, 1291–1314.
Yamamoto, T., Yokoyama, M., Opanasopit, P., Hayama, A., Kawano, K., Maitani, Y., 2007. What are determining factors for stable drug incorporation into polymeric micelle carriers? Consideration on physical and chemical characters of the micelle inner core. J. Contr. Rel. 123, 11–18.
Yokoyama, M., 2005. Polymeric micelles for the targeting of hydrophobic drugs. In: Kwon, G.S. (Ed.), Drug and Pharmaceutical Sciences, Polymeric Drug Delivery Systems, 148. Taylor & Francis, Boca Raton, pp. 533–575.
Yokoyama, M., 2007. Polymeric micelles as nano-sized drug carrier systems. In: Domb, A.J., Tabata, Y., Kumar, M.N.V.R., Farber, S. (Eds.), Nanoparticles for Pharmaceutical Applications. American Scientific Publishers, Stevenson Ranch, pp. 63–72.
Yokoyama, M., Opanasopit, P., Maitani, Y., Kawano, K., Okano, T., 2004. Polymer design and incorporation method for polymeric micelle carrier system containing water-insoluble anti-cancer agent camptothecin. J. Drug Target. 12, 373–384.
Yuan, F., Dellian, M., Fukumura, D., Leunig, M., Berk, D.A., Torchilin, V.P., Jain, R.K., 1995. Vascular permeability in a human tumor xenograft: molecular size dependence and cutoff size. Cancer Res. 55, 3752–3756.
Watanabe, M., Kawano, K., Yokoyama, M., Opanasopit, P., Okano, T., Maitani, Y., 2006. Preparation of camptothecin-loaded polymeric micelles and evaluation of their incorporation and circulation stability. Int. J. Pharm. 308, 183–189.

Please cite this article in press as: Shiraishi, K., et al., A facile preparation method of a PFC-containing nano-sized emulsion for theranostics of solid tumors. Int J Pharmaceut (2011), doi:10.1016/j.ijpharm.2011.10.006

molecular pharmaceutics

Article

pubs.acs.org/molecularpharmaceutics

Bubble Liposomes and Ultrasound Promoted Endosomal Escape of TAT-PEG Liposomes as Gene Delivery Carriers

Daiki Omata,[†] Yoichi Negishi,*[,†] Shoko Hagiwara,[†] Sho Yamamura,[†] Yoko Endo-Takahashi,[†] Ryo Suzuki,[‡] Kazuo Maruyama,[‡] Motoyoshi Nomizu,[§] and Yukihiko Aramaki[†]

[†]Department of Drug Delivery and Molecular Biopharmaceutics, School of Pharmacy, Tokyo University of Pharmacy and Life Sciences, Hachioji, Tokyo 192-0392, Japan

[‡]Department of Biopharmaceutics, School of Pharmaceutical Sciences, Teikyo University, Sagamihara, Kanagawa 252-5195, Japan

[§]Department of Clinical Biochemistry, School of Pharmacy, Tokyo University of Pharmacy and Life Sciences, Hachioji, Tokyo 192-0392, Japan

ABSTRACT: We have previously developed laminin-derived AG73 peptide-labeled poly(ethylene glycol)-modified liposomes (AG73-PEG liposomes) for selective cancer gene therapy and reported that Bubble liposomes (BLs) and ultrasound (US) exposure could accelerate the endosomal escape of AG73-PEG liposomes, leading to the enhancement of transfection efficiency; however, it is still unclear whether BLs and US exposure can also enhance the transfection efficiency of other vectors. We therefore assessed the effect of BLs and US exposure on the gene transfection efficiency of *trans*-activating transcriptor (TAT) peptide modified PEG liposomes. Although TAT-PEG liposomes were efficiently internalized into cells, the efficacy of endosomal escape was insufficient. The transfection efficiencies of TAT-PEG liposomes were enhanced by about 30-fold when BLs and US exposure were used. We also confirmed that BLs and US exposure could not enhance the direct transportation of TAT-PEG liposomes into cells. Confocal microscopy showed that BLs and US exposure promoted endosomal escape of TAT-PEG liposomes. Our results suggested that BLs and US exposure could enhance transfection efficiency by promoting endosomal escape, which was independent of modified molecules of carriers. Thus, BLs and US exposure can be a useful tool to achieve efficient gene transfection by improving endosomal escape of various carriers.

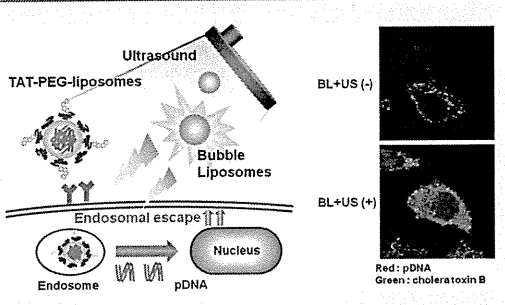

KEYWORDS: *Bubble liposomes, gene delivery, TAT peptide, ultrasound*

INTRODUCTION

Successful gene therapy depends on the efficient and safe delivery of genes into the desired tissues and cells. It is therefore necessary to develop efficient delivery vectors or methods for gene therapy. Nonviral vectors, such as cationic lipids or polymers, continue to be an attractive alternative to viral vectors due to their safety and convenient large-scale production, but their relatively low transfection efficiency compared with viral vectors is a major disadvantage.[1] In nonviral gene therapy, high transfection activity is required to improve the rate-limiting steps such as cellular internalization, endosomal escape, nuclear transfer, and intranuclear transcription.[2,3] In these steps, endosomal escape is considered one of the most important steps. When the vector cannot overcome this process, the cargo is degraded in lysosomes, leading to decreased gene transfection efficiency. For efficient endosomal escape, some studies have developed carriers equipped with functions such as pH sensitivity,[4,5] temperature dependence,[6] or photosensitivity.[7]

We have previously developed laminin-derived AG73 peptide-labeled poly(ethylene glycol) modified liposomes (AG73-PEG liposomes) for selective cancer gene therapy.[8] We also reported that echo-contrast gas-entrapping PEG liposomes, called "Bubble liposomes" (BLs), and ultrasound (US) exposure could accelerate the endosomal escape of AG73-PEG liposomes, leading to enhanced transfection efficiency.[9] It is expected that BLs and US exposure may promote the endosomal escape of various carriers and enhance their transfection efficiency; however, it is still unclear whether BLs and US exposure can enhance the transfection efficiency of vectors other than AG73-PEG liposomes, and the effect of BLs and US exposure on the transfection efficiency and endosomal escape of other functional molecule modified gene delivery carriers is not clearly understood.

Cell-penetrating peptides (CPPs), such as TAT and R8 peptides, are able to facilitate penetration through cell membranes and translocate different cargo into cells.[10] The TAT peptide, derived from a human immunodeficiency virus trans-acting transcriptional activator, has been studied to achieve highly efficient gene delivery and to develop TAT-modified liposomes and a polyplex.[11,12] The majority of these carriers were internalized via endocytosis and were required to achieve endosomal escape for efficient gene transfection.[13] Additionally, TAT-modified carriers equipped with components enhancing endosomal escape have been developed.[14]

Received: July 13, 2011
Revised: October 6, 2011
Accepted: October 24, 2011
Published: October 24, 2011

We therefore prepared TAT-modified liposomes as a model to evaluate the effect of BLs and US exposure on gene transfection efficiency via endosomal escape.

In this study, to assess the utility of BLs and US exposure for efficient gene delivery in general, we focused on TAT peptide and evaluated the effect of BLs and US exposure on the gene transfection efficiency of TAT-modified liposomes.

EXPERIMENTAL SECTION

Materials. The plasmid pCMV-Luc is an expression vector encoding the firefly luciferase gene under the control of cytomegalovirus promoter. Fluorescein isothiocyanate-conjugated cholera toxin B subunit (FITC-CTB), chloroquine, chlorpromazine and protamine were purchased from Sigma (St. Louis, MO). Cy3-labeled pDNA was purchased from Mirus Bio, LLC (Madison, WI). Genistein was purchased from Wako Pure Chemical Industries, Ltd. (Osaka, Japan). Amiloride was purchased from Calbiochem (San Diego, CA).

Cell Lines and Cultures. HeLa cells (human cervical cell line) were cultured in Dulbecco's modified Eagle's medium (DMEM; Kohjin Bio Co. Ltd., Tokyo, Japan), supplemented with 10% fetal bovine serum (FBS; Equitech Bio Inc., Kerrville, TX), penicillin (100 U/mL), and streptomycin (100 μg/mL) at 37 °C in a humidified 5% CO_2 atmosphere.

Preparation of TAT-PEG Liposomes. The Cys-TAT peptide (CGG-GRKKRRQRRRPPQ) was synthesized manually using the 9-fluorenylmethoxycarbonyl (Fmoc)-based solid-phase strategy, prepared in the COOH-terminal amide form and purified by reverse-phase high performance liquid chromatography. Liposomes were prepared by the hydration method. pDNA diluted in 10 mM HEPES buffer (pH 7.4) was condensed using protamine (N/P = 5.0). The complex of pDNA and protamine was added to a lipid film composed of 1,2-dioleoyl-*sn*-glycero-3-phospho-*rac*-1-glycerol (DOPG) (AVANTI Polar Lipids Inc., Alabaster, AL), 1,2-dioleoyl-*sn*-glycero-3-phosphoethanolamine (DOPE) (AVANTI Polar Lipids, Inc.), and 1,2-distearoyl-*sn*-glycero-3-phophatidylethanolamine-polyethyleneglycol-maleimide (DSPE-PEG_{2000}-Mal) (NOF Corporation, Tokyo, Japan) in a molar ratio of 2:9:0.57, followed by incubation for 10 min at room temperature to hydrate the lipids. The solution was sonicated for 5 min in a bath-type sonicator (42 kHz, 100 W) (2510J-DTH; Bransonic Ultrasonic Co., Danbury, CT). For coupling, TAT peptide, at a molar ratio of 5-fold DSPE-PEG_{2000}-Mal, was added to the PEG liposomes, and the mixture was incubated for 6 h at room temperature to conjugate the cysteine of the Cys-TAT peptide with the maleimide of the PEG liposomes using a thioether bond. The resulting TAT-peptide conjugated PEG liposomes (TAT-PEG liposomes) were dialyzed to remove any excess peptide. TAT-PEG liposomes were modified with 5 mol % PEG and 3 mol % peptides of total lipid. The particle size and ζ-potential of prepared liposomes were measured by NICOMP 380 ZLS (Particle Sizing Systems, Santa Barbara, CA).

Preparation of Bubble Liposomes. PEG liposomes composed of 1,2-dipalmitoyl-*sn*-glycero-3-phosphocholine (DPPC) (NOF Corporation) and 1,2-distearoyl-*sn*-glycero-3-phosphatidylethanolamine-poly(ethylene glycol) (DSPE-PEG_{2000}-OMe) (NOF Corporation) in a molar ratio of 94:6 were prepared by the reverse-phase evaporation method. In brief, all reagents were dissolved in 1:1 (v/v) chloroform/diisopropyl ether. Phosphate-buffered saline was added to the lipid solution, and the mixture was sonicated and then evaporated at 47 °C. The organic solvent was completely removed, and the size of the liposomes was adjusted to less than 200 nm using extruding equipment and a sizing filter (pore size: 200 nM) (Nuclepore Track-Etch Membrane; Whatman Plc, UK). The lipid concentration was measured using a phospholipid C test Wako (Wako Pure Chemical Industries, Ltd., Osaka, Japan). BLs were prepared from liposomes and perfluoropropane gas (Takachio Chemical Ind. Col. Ltd., Tokyo, Japan). First, 2 mL sterilized vials containing 0.8 mL of liposome suspension (lipid concentration: 1 mg/mL) were filled with perfluoropropane gas, capped, and then pressurized with a further 3 mL of perfluoropropane gas. The vial was placed in a bath-type sonicator (42 kHz, 100 W) (2510j-DTH; Branson Ultrasonics Co.) for 5 min to form BLs.

Transfection of pDNA into Cells Using TAT-PEG Liposomes. The day before the experiments, HeLa cells (3×10^4) were seeded in a 48-well plate. The cells were treated with TAT-PEG liposomes (encapsulated pDNA: 3 μg/mL) in serum-free medium for 4 h at 37 °C. After replacement with fresh medium, the cells were cultured for 20 h, and then luciferase activity was measured.

Transfection of pDNA into Cells by Combination of TAT-PEG Liposomes with BLs and US Exposure. The day before the experiments, HeLa cells (3×10^4) were seeded in a 48-well plate. The cells were treated with TAT-PEG liposomes (encapsulated pDNA: 3 μg/mL) in serum-free medium for 4 h at 37 °C. After incubation, the cells were washed twice within 10 min to remove any excess TAT-PEG liposomes that were not associated with the cells, and BLs (120 μg/mL) were added. Within 2 min, US exposure was applied through a 6 mm diameter probe placed in the well (frequency, 2 MHz; duty, 50%; burst rate, 2 Hz; intensity, 1.0 W/cm^2; time, 10 s). A Sonopore 3000 (NEPA GENE Co. Ltd., Chiba, Japan) was used to generate the US exposure. The cells were cultured for 20 h; then luciferase activity was determined, and cell viability was measured using a WST-8 assay (Cell Counting Kit-8; Dojindo Laboratories, Kumamoto, Japan).

Measurement of Luciferase Expression. Cell lysate was prepared with lysis buffer (0.1 M Tris-HCl (pH 7.8), 0.1% Triton X-100, and 2 mM EDTA). Luciferase activity was measured using a luciferase assay system (Promega) and a luminometer (LB96 V; Berthold Japan Co. Ltd., Tokyo, Japan). Activity is indicated as relative light units (RLU) per milligrams of protein.

Flow Cytometry Analysis. The day before the experiments, HeLa cells were seeded in a 12-well plate. Then, 0.2 mol % DiI-labeled TAT-PEG liposomes (pDNA: 3 μg/mL) were added to the cells and incubated for 1 h at 37 °C. The cells were collected, and the fluorescence intensities were measured by flow cytometry (FACSCanto; BD Biosciences, Franklin Lakes, NJ) to evaluate the cellular association of liposomes.

To examine the effect of BLs and US exposure on cellular uptake of pDNA, TAT-PEG liposomes (encapsulating Cy3-labeled pDNA: 3 μg/mL) were added to cells and incubated for 4 h at 37 °C. After incubation, the cells were washed twice, and BLs (120 μg/mL) were added. Then, US exposure was applied (frequency, 2 MHz; duty, 50%; burst rate, 2 Hz; intensity, 1.0 W/cm^2; time, 10 s). Subsequently, the cells were incubated for 10 or 60 min, and then the cells were collected by trypsinization and washed with PBS supplemented with heparin (50 μg/mL) three times to remove TAT-PEG liposomes and pDNA bound to the cell surface. The fluorescence intensity was measured by flow cytometry.

Confocal Laser Scanning Microscopy (CLSM). HeLa cells were seeded a day before the experiments. HeLa cells were

dx.doi.org/10.1021/mp200353m | *Mol. Pharmaceutics* 2011, 8, 2416–2423